2020 2nd Season Stock Assessment

Falkland calamari

(*Doryteuthis gahi*)

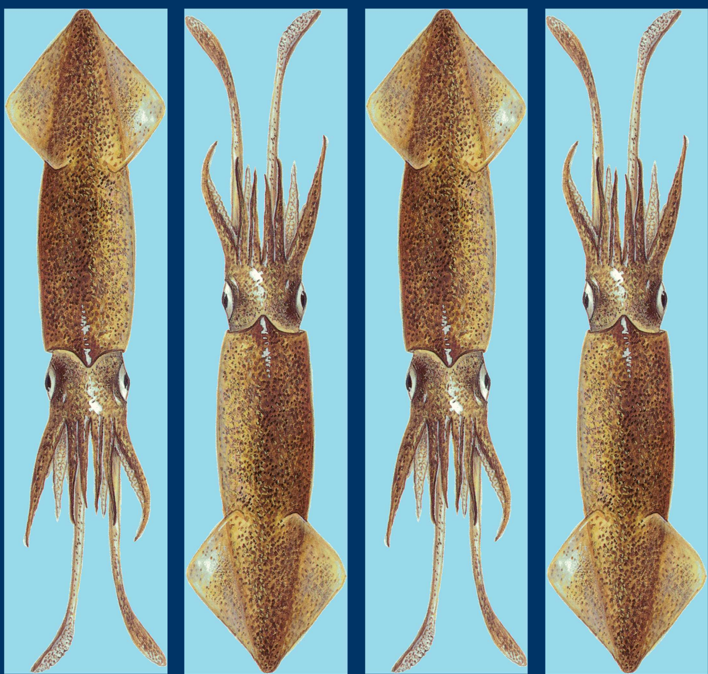

S2 - 2020 - LOL

Andreas Winter

Natural Resources - Fisheries
Falkland Islands Government
Stanley, Falkland Islands

November 2020

Index

Summary

1) The 2020 second season *Doryteuthis gahi* fishery (X license) was open from July 30th and closed by directed order on October 1st. Compensatory days for operational matters and bad weather resulted in 48 vessel-days taken after October 1st, with one vessel fishing as late as October 6th.
2) 29,759 tonnes of *D. gahi* catch were reported in the 2020 X-license fishery, giving an average CPUE of 30.0 t vessel-day^{-1}. Both catch and CPUE were above median for second seasons. 59.2% of *D. gahi* catch and 57.6% of fishing effort were taken south of 52º S; 40.8% of *D. gahi* catch and 42.4% of fishing effort were taken north of 52º S.
3) In the south sub-area, two depletion periods / immigrations were inferred to have started on July 30th (start of the season), and September 6th. In the north sub-area, two depletion periods / immigrations were inferred to have started on July 30th and August 19th.
4) Approximately 11,022 tonnes of *D. gahi* (95% confidence interval: 3,405 to 18,511 t) were estimated to have immigrated into the Loligo Box after the start of second season 2020, of which 3,454 t south of 52º S and 7,568 t north of 52º S.
5) The escapement biomass estimate for *D. gahi* remaining in the Loligo Box at the end of second season 2020 was: Maximum likelihood of 11,867 tonnes, with a 95% confidence interval of 8,855 to 19,744 tonnes.
   The risk of *D. gahi* escapement biomass at the end of the season being less than 10,000 tonnes was estimated at 8.8%.

Introduction

The second season (X licence) of the 2020 *Doryteuthis gahi* fishery (Patagonian longfin squid – colloquially *Loligo*) opened on July 30th; a one-day delay occasioned by the logistic difficulties of requiring marine mammal observers transported to the Falkland Islands by military flight. Ultimately, marine mammal observers could not be released from quarantine in time to join season opening, and the arrangement was made for X licence vessels to return to port on August 6th to pick up their observer. This interruption was credited as an extra flex day, with the usual provision (FIFD / LPG 2017) that vessels could not carry out other commercial or operational activities[a]. Thirteen vessels took August 6th as a flex day. Throughout the rest of the season, one vessel delayed entry to complete crew health tests in Stanley, and one vessel was replaced for 7 days from the start of the season to complete mechanical repairs. A total of 43 flex days were taken for bad weather, of which 14 on August 30th, 16 on September 19th, and 13 on September 20th (Figure 1). This season may also have set a record – of sorts – for reversed decisions; with 6 vessels requesting bad weather days on August 31st, then cancelling, 10 vessels requesting bad weather days on September 17th, then cancelling, and 1 vessel cancelling on September 20th. The season ended by directed closure on October 1st, and the various schedule flex adjustments amounted to 48 vessel-days deferred after October 1st. The last vessel finished fishing on October 6th.

Total reported *D. gahi* catch under second season X licence was 17,609 south + 12,150 north = 29,759 tonnes (Table 1), corresponding to an average CPUE of 29759 / 993 = 30.0 tonnes vessel-day^{-1}. Both catch and average CPUE were above the median for second seasons since 2004.

[a] Except to land medical casualties.

Figure 1 [below]. Fish Ops chart display and wind speed vector plots (Copernicus Marine Service) on August 30th, when only two vessels fished, September 19th, when no vessels fished, and September 20th, when only two vessels fished.

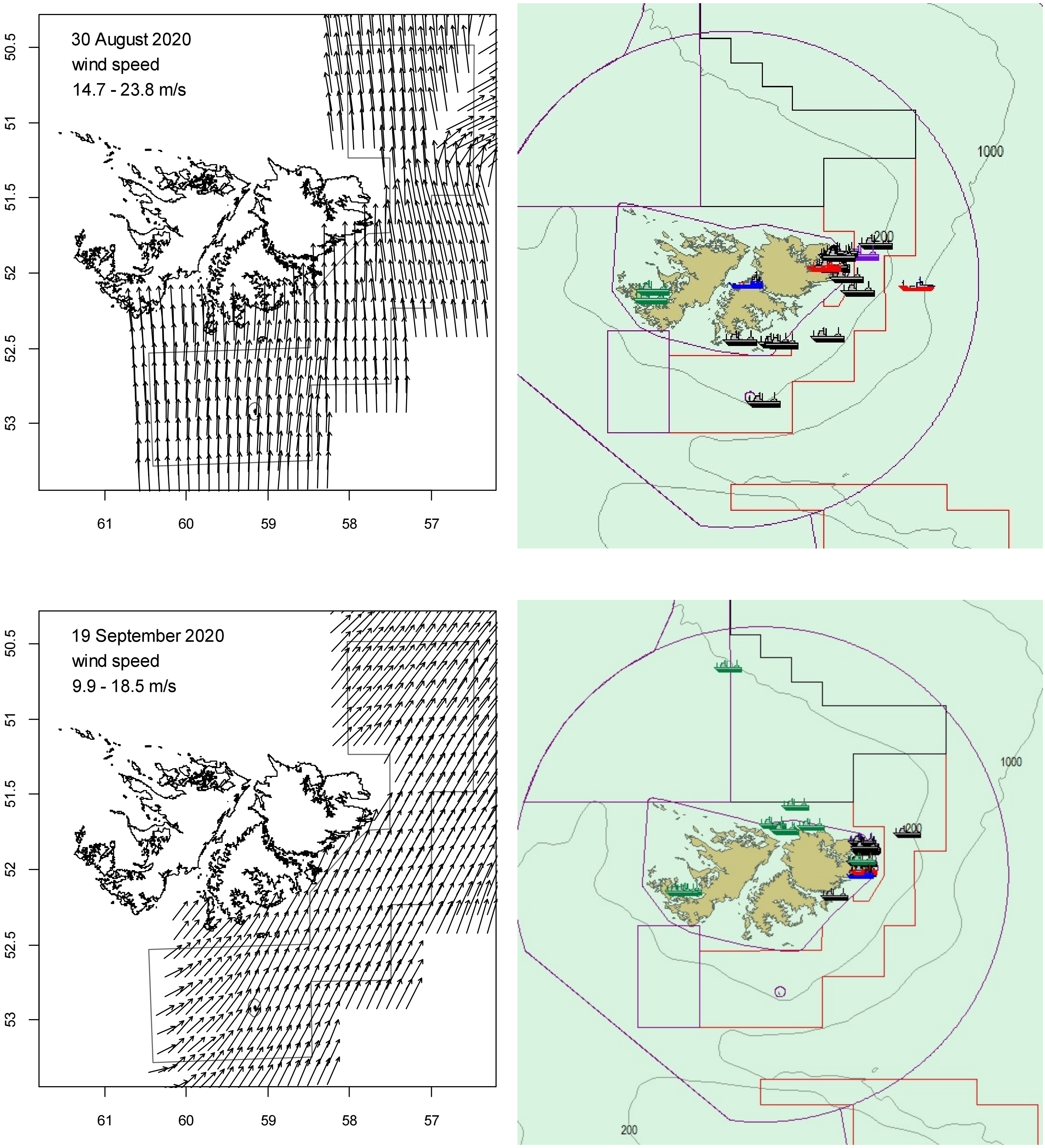

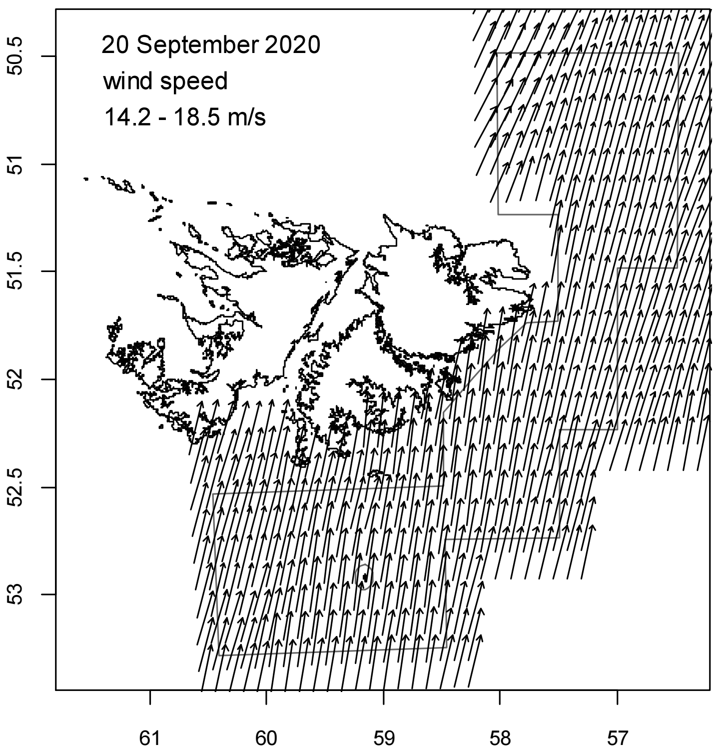

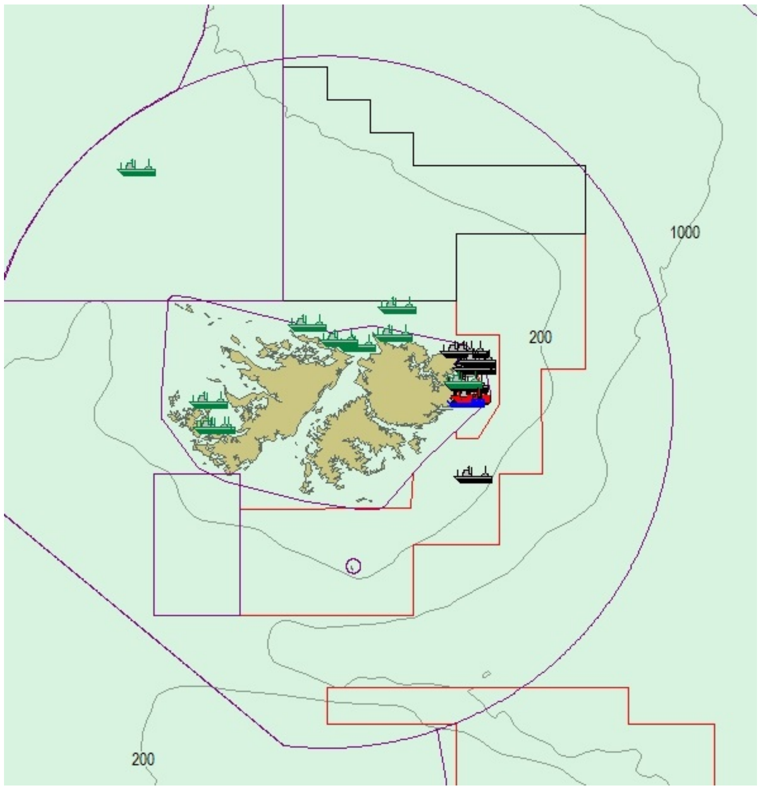

Table 1. *D. gahi* season comparisons since 2004, when catch management was assumed by the FIFD. Days: total number of calendar days open to licensed *D. gahi* fishing including (since 1st season 2013) optional extension days; V-Days: aggregate number of licensed *D. gahi* fishing days reported by all vessels for the season. Entries in italics are seasons closed by emergency order.

	Season 1			Season 2		
	Catch (t)	Days	V-Days	Catch (t)	Days	V-Days
2004	7,152	46	625	17,559	78	1271
2005	24,605	45	576	29,659	78	1210
2006	19,056	50	704	*23,238*	*53*	*883*
2007	17,229	50	680	*24,171*	*63*	*1063*
2008	24,752	51	780	26,996	78	1189
2009	12,764	50	773	*17,836*	*59*	*923*
2010	28,754	50	765	36,993	78	1169
2011	15,271	50	771	*18,725*	*70*	*1099*
2012	34,767	51	770	35,026	78	1095
2013	19,908	53	782	19,614	78	1195
2014	28,119	59	872	19,630	71	1099
2015	*19,383**	*57**	*871**	*10,190*	*42*	*665*
2016	22,616	68	1020	23,089	68	1004
2017	39,433	68	999†	24,101	69	1002‡
2018	43,085	69	975	35,828	68	977
2019	55,586	68	953	*24,748*	*43*	*635*
2020	29,116	68	1012	29,759	69	993

* Does not include C-license catch or effort after the C-license target for that season was switched from *D. gahi* to *Illex*.

† Includes two vessel-days of experimental fishing for juvenile toothfish.

‡ Includes one vessel-day of experimental fishing for juvenile toothfish.

The particular circumstance of season opening without marine mammal observers led to the agreement that all vessels fished with Seal Exclusion Devices (SEDs) (Iriarte et al. 2020) until they could pick up their observer; on August 6th. With observers embarked, the requirement for SEDs was lifted and vessels resumed fishing on August 7th. Hours later, six pinniped mortalities had been reported from the south sub-area of the Loligo Box (south of 52°), and the use of SEDs was reinstated in the south with immediate effect. By noon, a pinniped mortality had been reported from the north sub-area, and the use of SEDs was reinstated in the north with effect from the start of August 8th. Of 60 X-licence trawls in the water on August 7th, 28 were equipped with a SED (some in the north voluntarily), and this season overall presented the most comprehensive mandate for SEDs since the start of the pinniped problem in 2017.

Assessment of the Falkland Islands *D. gahi* stock was conducted with depletion time-series models as in previous seasons (Agnew et al. 1998, Roa-Ureta and Arkhipkin 2007; Arkhipkin et al. 2008), and in other squid fisheries (cited in Arkhipkin et al. 2020). Because *D. gahi* has an annual life cycle (Patterson 1988, Arkhipkin 1993), stock cannot be derived from a standing biomass carried over from prior years (Rosenberg et al. 1990, Pierce and Guerra 1994). The depletion model instead calculates an estimate of population abundance over time by evaluating what levels of abundance and catchability must be present to sustain the observed rate of catch. Depletion modelling of the *D. gahi* target fishery is used both in-season and for the post-season summary, with the objective of maintaining an escapement biomass of 10,000 tonnes *D. gahi* at the end of each season as a conservation threshold (Agnew et al. 2002, Barton 2002).

Methods

The depletion model formulated for the Falklands *D. gahi* stock is based on the equivalence:

$$C_{day} = q \times E_{day} \times N_{day} \times e^{-M/2} \qquad \textbf{(1)}$$

where q is the catchability coefficient, M is the natural mortality rate (considered constant at 0.0133 day^{-1}; Roa-Ureta and Arkhipkin 2007), and C_{day}, E_{day}, N_{day} are respectively catch (numbers of squid), fishing effort (numbers of vessels), and abundance (numbers of squid) per day. In its basic form (DeLury 1947) the depletion model assumes a closed population in a fixed area for the duration of the assessment. However, the assumption of a closed population is imperfectly met in the Falkland Islands fishery, where stock analyses have often shown that *D. gahi* groups arrive in successive waves after the start of the season (Roa-Ureta 2012; Winter and Arkhipkin 2015). Arrivals of successive groups are inferred from discontinuities in the catch data. Fishing on a single, closed cohort would be expected to yield gradually decreasing CPUE, but gradually increasing average individual sizes, as the squid grow. When instead these data change suddenly, or in contrast to expectation, the immigration of a new group to the population is indicated (Winter and Arkhipkin 2015).

In the event of a new group arrival, the depletion calculation must be modified to account for this influx. This is done using a simultaneous algorithm that adds new arrivals on top of the stock previously present, and posits a common catchability coefficient for the entire depletion time-series. If two depletions are included in the same model (i.e., the stock present from the start plus a new group arrival), then:

$$C_{day} = q \times E_{day} \times (N1_{day} + (N2_{day} \times i2\big|_0^1)) \times e^{-M/2} \qquad \textbf{(2)}$$

where i2 is a dummy variable taking the values 0 or 1 if 'day' is before or after the start day of the second depletion. For more than two depletions, $N3_{day}$, i3, $N4_{day}$, i4, etc., would be included following the same pattern.

In several previous seasons since second season 2017 (Winter 2017), the depletion equation **(2)** was further modified to differentiate between catches taken with or without SEDs installed in the trawl nets. However, an analysis computed last year (Winter 2019a) found that daily biomass estimation did not change significantly between implementation or not of SED differentiation, and this modification was discontinued (Winter 2019b). All catch efficiencies, with or without SED, are considered part of the fleet's overall range of variation.

The season depletion likelihood function was calculated as the difference between actual catch numbers reported and catch numbers predicted from the model (Equation **2**), statistically corrected by a factor relating to the number of days of the depletion period (Roa-Ureta 2012):

$$\text{minimization} \rightarrow \quad \left(\left(n\text{Days - 2}\right)/2\right) \times \log\left(\sum_{days}\left(\log\left(\text{predicted } C_{\text{day}}\right) - \log\left(\text{actual } C_{\text{day}}\right)\right)^2\right) \quad \textbf{(3)}$$

The stock assessment was set in a Bayesian framework (Punt and Hilborn 1997), whereby results of the season depletion model are conditioned by prior information on the stock; in this case the information from the pre-season survey.

The likelihood function of prior information was calculated as the normal distribution of the difference between catchability (q) derived from the survey abundance estimate, and catchability derived from the season depletion model. Applying this difference requires both the survey and the season to be fishing the same stock with the same gear. Catchability, rather than abundance N, is used for calculating prior likelihood because catchability informs the entire season time series; whereas N from the survey only informs the first in-season depletion period – subsequent immigrations and depletions are independent of the abundance that was present during the survey. Thus, the prior likelihood function was:

$$\text{minimization} \rightarrow \quad \frac{1}{\sqrt{2\pi \cdot \mathrm{SD}_{\mathrm{q\ prior}}{}^2}} \times \exp\left(-\frac{\left(\mathrm{q}_{\mathrm{model}} - \mathrm{q}_{\mathrm{prior}}\right)^2}{2 \cdot \mathrm{SD}_{\mathrm{q\ prior}}{}^2}\right) \quad \textbf{(4)}$$

where the standard deviation of catchability prior ($\mathrm{SD}_{\mathrm{q\ prior}}$) was calculated from the Euclidean sum of the survey prior estimate uncertainty, the variability in catches on the season start date, and the uncertainty in the natural mortality M estimate over the number of days mortality discounting (Appendix: Equations **A5-S**, **A5-N**).

Bayesian optimization of the depletion was calculated by jointly minimizing Equations **3** and **4**, using the Nelder-Mead algorithm in R programming package 'optimx' (Nash and Varadhan 2011). Relative weights in the joint optimization were assigned to Equations **3** and **4** as the converse of their coefficients of variation (CV), i.e., the CV of the prior became the weight of the depletion model and the CV of the depletion model became the weight of the prior. Calculations of the depletion CVs are described in Equations **A8-S** and **A8-N**. Because a complex model with multiple depletions may converge on a local minimum rather than global minimum, the optimization was stabilized by running a feed-back loop that set the q and N parameter outputs of the Bayesian joint optimization back into the in-season-only minimization (Equation **3**), re-calculated this minimization and the CV resulting from it, then re-calculated the Bayesian joint optimization, and continued this process until both the in-season minimization and the joint optimization remained unchanged.

With actual C_{day}, E_{day} and M being fixed parameters, the optimization of Equation **2** using Equations **3** and **4** produces estimates of q and N1, N2, …, etc. Numbers of squid on the final day (or any other day) of a time series are then calculated as the numbers N of the depletion start days discounted for natural mortality during the intervening period, and subtracting cumulative catch also discounted for natural mortality (CNMD). Taking for example a two-depletion period:

$$
\begin{aligned}
N_{\text{final day}} = \; & N1_{\text{start day 1}} \times e^{-M\,(\text{final day} - \text{start day 1})} \\
& + N2_{\text{start day 2}} \times e^{-M\,(\text{final day} - \text{start day 2})} \\
& - CNMD_{\text{final day}}
\end{aligned}
\qquad \textbf{(5)}
$$

where

$$CNMD_{\text{day 1}} = 0$$

$$CNMD_{\text{day x}} = CNMD_{\text{day x-1}} \times e^{-M} + C_{\text{day x-1}} \times e^{-M/2} \qquad \textbf{(6)}$$

$N_{\text{final day}}$ is then multiplied by the average individual weight of squid on the final day to give biomass. Daily average individual weight is obtained from length / weight conversion of mantle lengths measured in-season by observers, and also derived from in-season commercial data as the proportion of product weight that vessels reported per market size category. Observer mantle lengths are scientifically accurate, but restricted to 1-2 vessels at any one time that may or may not be representative of the entire fleet, and not available every day. Commercially proportioned mantle lengths are relatively less accurate, but cover the entire fishing fleet every day. Therefore, both sources of data are used (see Appendix – *Doryteuthis gahi* individual weights).

Distributions of the likelihood estimates from joint optimization (i.e., measures of their statistical uncertainty) were computed using a Markov Chain Monte Carlo (MCMC) (Gamerman and Lopes 2006), a method that is commonly employed for fisheries assessments (Magnusson et al. 2013). MCMC is an iterative process which generates random stepwise changes to the proposed outcome of a model (in this case, the q and N of *D. gahi* squid) and at each step, accepts or nullifies the change with a probability equivalent to how well the change fits the model parameters compared to the previous step. The resulting sequence of accepted or nullified changes (i.e., the 'chain') approximates the likelihood distribution of the model outcome. The MCMC of the depletion models were run for 200,000 iterations; the first 1000 iterations were discarded as burn-in sections (initial phases over which the algorithm stabilizes); and the chains were thinned by a factor equivalent to the maximum of either 5 or the inverse of the acceptance rate (e.g., if the acceptance rate was 12.5%, then every 8^{th} (0.125^{-1}) iteration was retained) to reduce serial correlation. For each model three chains were run; one chain initiated with the parameter values obtained from the joint optimization of Equations **3** and **4**, one chain initiated with these parameters ×2, and one chain initiated with these parameters ×¼. Convergence of the three chains was accepted if the variance among chains was less than 10% higher than the variance within chains (Brooks and Gelman 1998). When convergence was satisfied the three chains were combined as one final set. Equations **5**, **6**, and the multiplication by average individual weight were applied to the CNMD and each iteration of N values in the final set, and the biomass outcomes from these calculations represent the distribution of the estimate. The peaks of the MCMC histograms were compared to the empirical optimizations of the N values.

Depletion models and likelihood distributions were calculated separately for north and south sub-areas of the Loligo Box fishing zone, as *D. gahi* sub-stocks emigrate from different spawning grounds and remain to an extent segregated (Arkhipkin and Middleton 2002). Total escapement biomass is then defined as the aggregate biomass of *D. gahi* on the last day of the season for north and south sub-areas combined. North and south biomasses are not assumed to be uncorrelated however (Shaw et al. 2004), and therefore north and south likelihood distributions were added semi-randomly in proportion to the strength of their day-to-day correlation (see Winter 2014, for the semi-randomization algorithm).

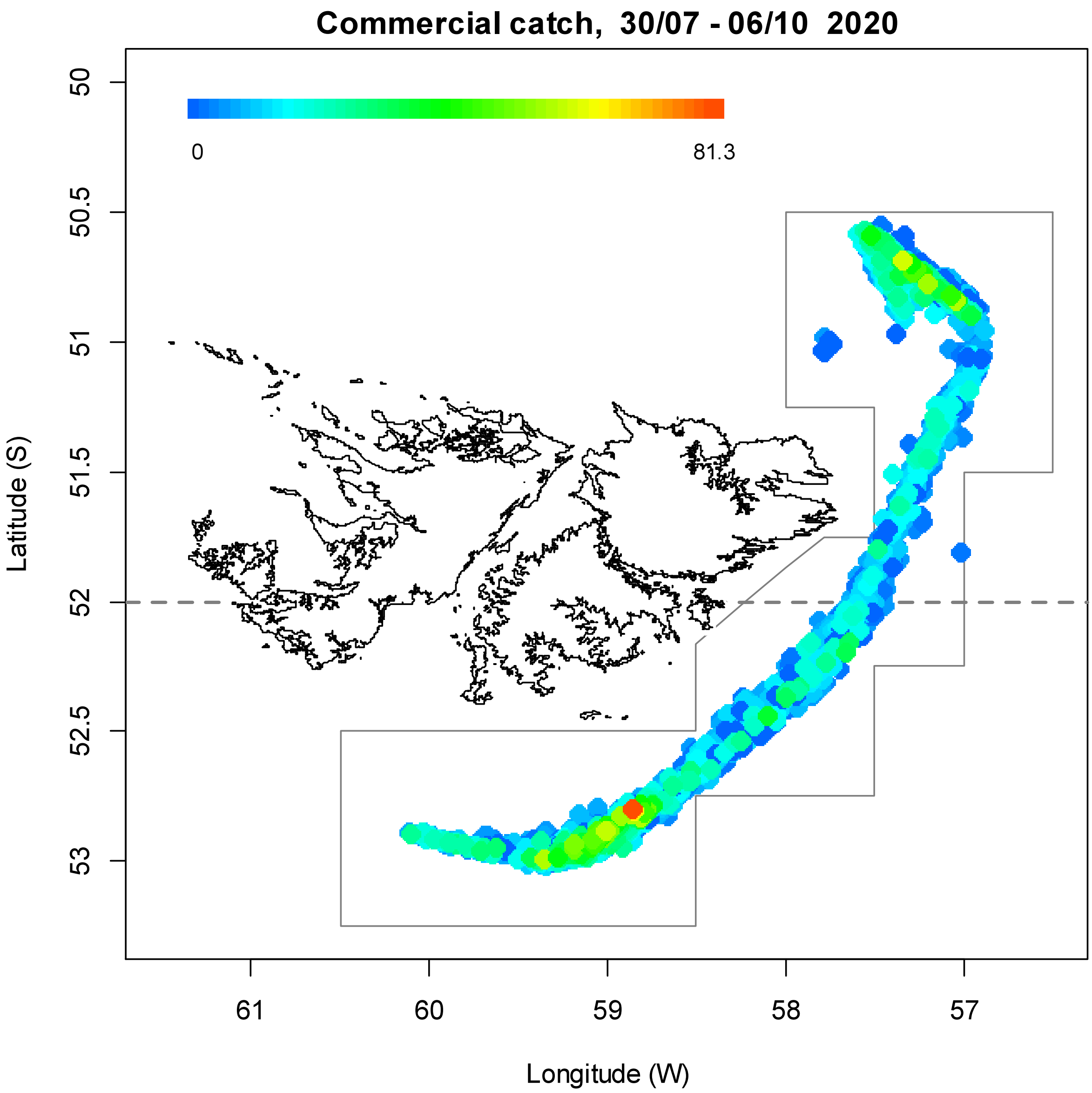

Figure 2. Spatial distribution of *D. gahi* 2nd-season trawls, colour-scaled to catch weight (max. = 81.3 tonnes). 3317 trawl catches were taken during the season. The 'Loligo Box' fishing zone and 52 °S parallel delineating the boundary between north and south assessment sub-areas, are shown in grey.

Stock assessment

The north sub-area was fished on 63 of 69 season-days, for 40.8% of total catch (12150.1 t *D. gahi*) and 42.4% of effort (421.1 vessel-days) (Figures 2 and 3). The south sub-area was fished on 65 of 69[b] season-days, for 59.2% of total catch (17609.3 t *D. gahi*) and 57.6% of effort (571.9 vessel-days). 35.9% of south catch, vs. 14.9% of south effort, was taken in the first 7 days before the observer pick-up, underlining a highly concentrated season beginning. Throughout the season *D. gahi* catch distribution was again notably centric (Figure 2), with 10.6% of total catch taken between 52°S and 52.5°S; the historically defined central sub-area of the Loligo Box (e.g., Figure 2 in Roa-Ureta and Arkhipkin 2007).

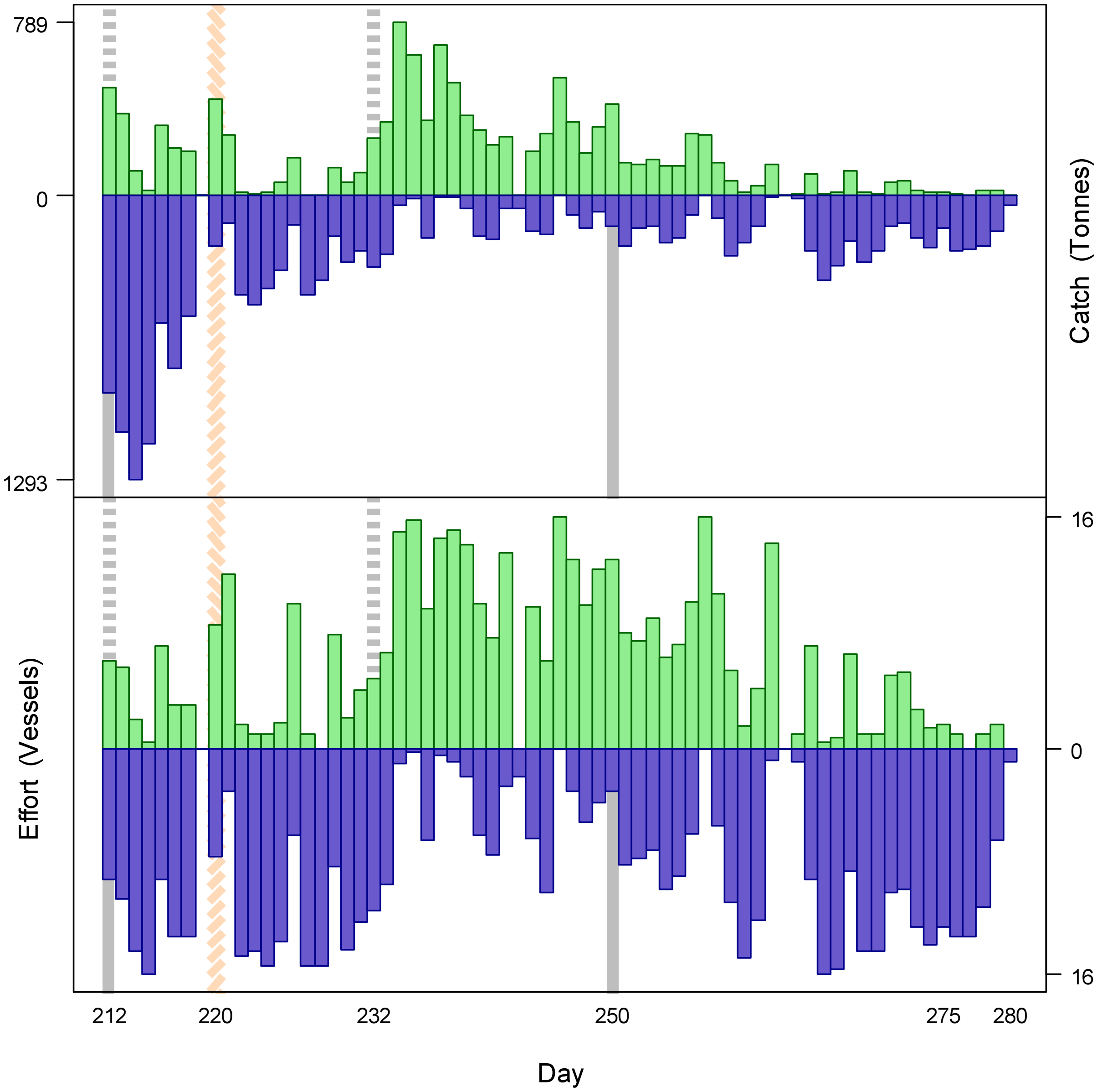

Figure 3. Daily total *D. gahi* catch and effort distribution by assessment sub-area north (green) and south (purple) of the 52° S parallel during 2nd season 2020. The season was open from July 30th (chronological day 212) to October 1st (chronological day 275), plus flex days until October 6th (day 280). Orange striping delineates the one day (August 7th, day 220) that SEDs were <u>not</u> comprehensively mandated in the fishery. As many as 16 vessels fished per day north; as many as 16 vessels fished per day south. As much as 789 tonnes *D. gahi* was caught per day north; as much as 1293 tonnes *D. gahi* was caught per day south.

[b] Of which two days were not fished at all; one for observer pick-up and one for bad weather.

Data

993 vessel-days were fished during the season (Table 1), with a median of 16 vessels per day (mean 14.77) except for flex and weather extensions. Vessels reported daily catch totals to the FIFD and electronic logbook data that included trawl times, positions, depths, and product weight by market size categories. Three FIG fishery observers were deployed on five vessels in the fishing season for a total of 66 sampling days[c] (Brewin 2020, Evans 2020, Matošević 2020a, b, c). Throughout the 69 days of the season, 14 days had no FIG fishery observer covering, 44 days had 1 FIG fishery observer covering, and 11 days had two FIG fishery observers covering. Except for seabird days FIG fishery observers were tasked with sampling 200 *D. gahi* at two stations; reporting their maturity stages, sex, and lengths to 0.5 cm. Contract marine mammal monitors were tasked with measuring 200 unsexed lengths of *D. gahi* per day. The length-weight relationship for converting observer and commercially proportioned lengths was combined from 2nd pre-season and season length-weight data of both 2019 and 2020, as 2020 data became available progressively with on-going observer coverage. The final parameterization of the length-weight relationship included 3383 measures from 2019 and 6122 measures from 2020, giving:

$$\text{weight (kg)} \quad = \quad 0.16617 \times \text{length (cm)}^{2.20690} / 1000 \qquad \textbf{(7)}$$

with a coefficient of determination R^2 = 94.8%.

Group arrivals / depletion criteria

Start days of depletions - following arrivals of new *D. gahi* groups - were judged primarily by daily changes in CPUE, with additional information from sex proportions, maturity, and average individual squid sizes. CPUE was calculated as metric tonnes of *D. gahi* caught per vessel per day. Days were used rather than trawl hours as the basic unit of effort. Commercial vessels do not trawl standardized duration hours, but rather durations that best suit their daily processing requirements. An effort index of days is therefore more consistent.

Two days in the south and two days in the north were identified that represented the onset of separate immigrations / depletions throughout the season.

- The first depletion start south was set on day 212 (July 30th), the first day of the season with nine vessels fishing south. Average individual *D. gahi* weights were at the low end of their season trends (Figure 4A, 4B), and average CPUE was near its maximum for the season (Figure 5).
- The second depletion start south was identified on day 250 (September 6th). CPUE showed its highest peak since August 4th (albeit by just 3 vessels; Figure 5), and observer average individual weights achieved a minimum for the season (Figure 4B). Contrastingly, commercial average individual weights were at a local maximum (Figure 4A).
- The first depletion start north was set on day 212, the first day of the season with six vessels fishing north. Average CPUE was at the maximum for the season (Figure 5).
- The second depletion start north was identified on day 232 (August 19th) with a sharp increase in CPUE that persisted for three days (Figure 5). Commercial average individual weights were near a local minimum plateau (Figure 4A).

[c] Not counting seabird days (every fourth day).

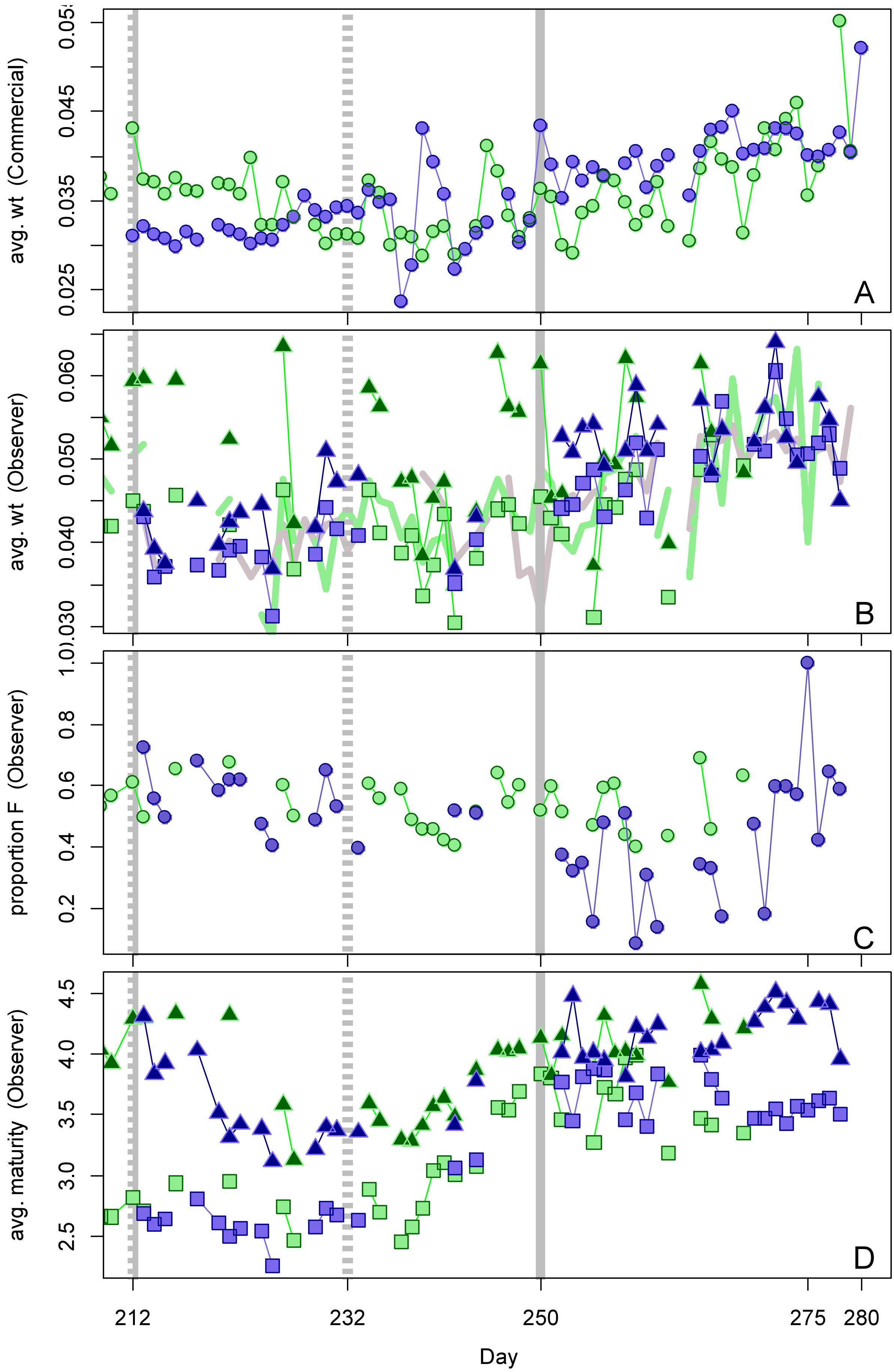

avg. wt (Commercial)
0.025
0.035
0.045
0.05
A
avg. wt (Observer)
0.030
0.040
0.050
0.060
B
proportion F (Observer)
0.2
0.4
0.6
0.8
1.0
C
avg. maturity (Observer)
2.5
3.0
3.5
4.0
4.5
D
212
232
250
275
280
Day

Figure 4 [previous page]. A: Average individual *D. gahi* weights (kg) per day from commercial size categories. B: Average individual *D. gahi* weights (kg) by sex per day from observer sampling. C: Proportions of female *D. gahi* per day from observer sampling. D: Average maturity value by sex per day from observer sampling. Males: triangles, females: squares, unsexed: circles. North sub-area: green, south sub-area: purple. Data from consecutive days are joined by line segments. Broken grey bars: the starts of in-season depletions north. Solid grey bars: the starts of in-season depletions south.

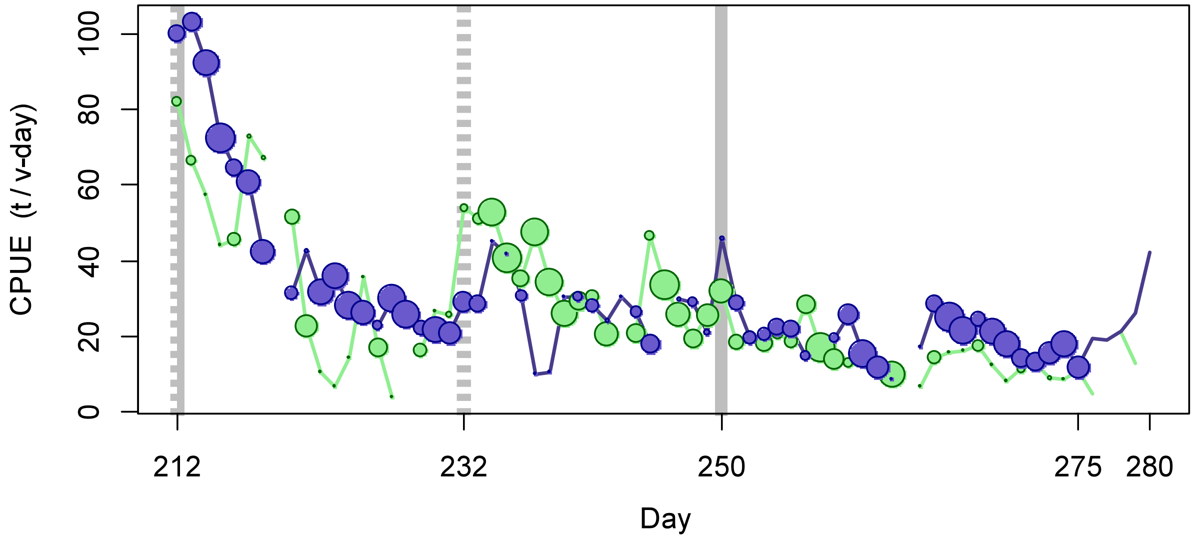

Figure 5. CPUE in metric tonnes per vessel per day, by assessment sub-area north (green) and south (purple) of 52° S latitude. Circle sizes are proportioned to numbers of vessels fishing. Data from consecutive days are joined by line segments. Broken grey bars indicate the starts of in-season depletions north. Solid grey bars indicate the starts of in-season depletions south.

Average CPUE obtained resurgences north and south also following the acute bad weather days on September 19th and 20th (Figure 1, Figure 5), and these CPUE changes were accompanied by short-term increases in average individual weight (Figures 4A, B). However, longer-term weight trends showed these changes to be relatively minor fluctuations. Average individual weight data on September 20th were from single vessels fishing in each of the north and south sub-areas (Figure 3), and suggest that a sorting effect of squid might have occurred in the presumably sloshing fish tanks, akin to sediment size-sorting in hydrological flows (Powell 1998). The corresponding days were therefore not identified as further immigrations / depletion starts.

Depletion analyses
South

In the south sub-area, Bayesian optimization was weighted nearly equally between in-season depletion at 0.597 (**A5-S**) and the prior at 0.585 (**A8-S**). The maximum likelihood posterior ($_{\text{Bayesian}}\, q_S = 2.394 \times 10^{-3}$; Figure 6-left, and Equation **A9-S**) was however closer to the pre-season prior ($_{\text{prior}}\, q_S = 2.667 \times 10^{-3}$; Figure 6-left, and Equation **A4-S**) than to the in-season depletion ($_{\text{depletion}}\, q_S = 1.360 \times 10^{-3}$; Figure 6-left, and **A6-S**), indicative that the in-season depletion model was relatively insensitive to catchability.

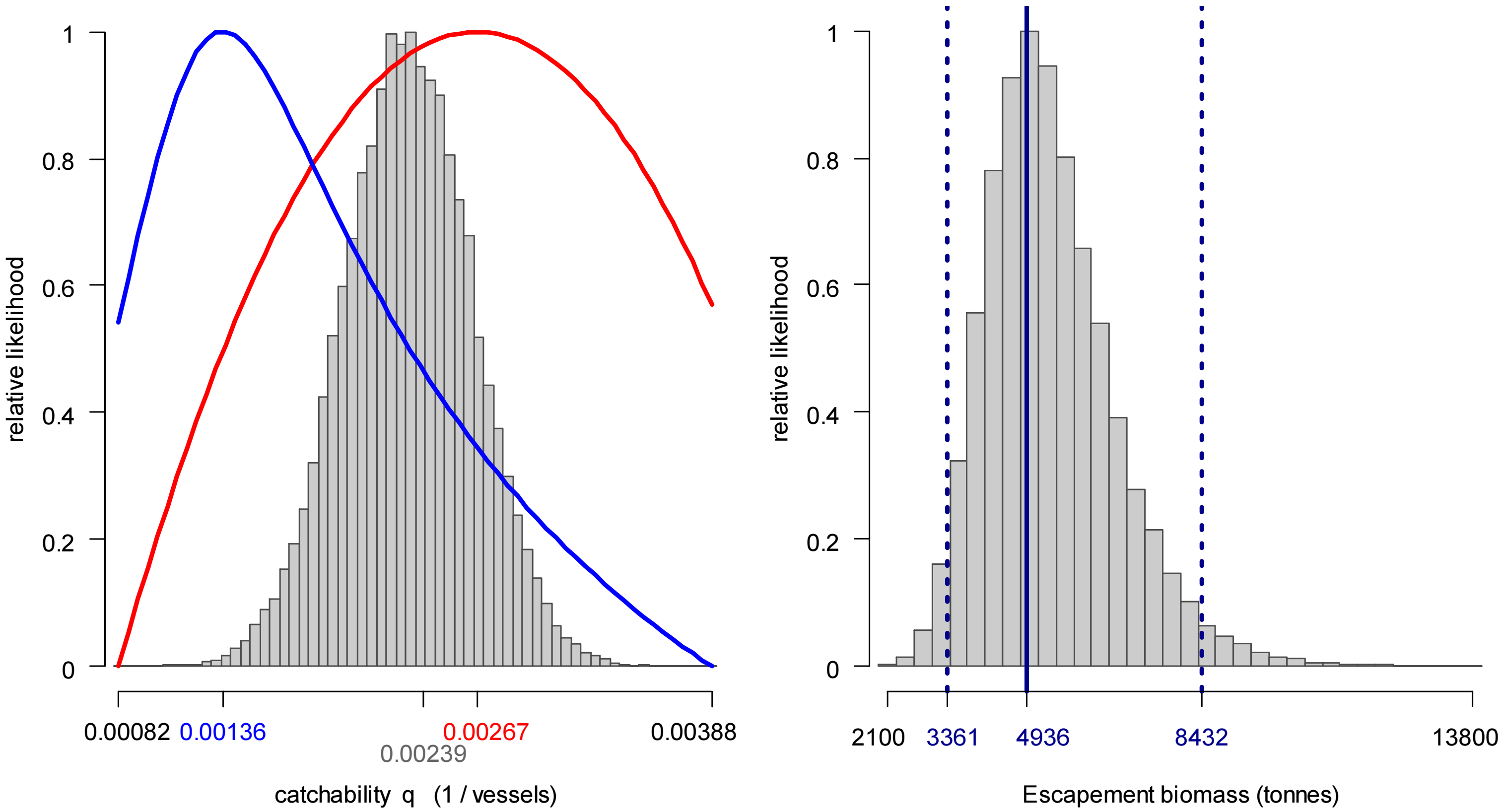

Figure 6. South sub-area. Left: Likelihood distributions for *D. gahi* catchability. Red line: prior model (pre-season survey data), blue line: in-season depletion model, grey bars: combined Bayesian model posterior. Right: Likelihood distribution (grey bars) of escapement biomass, from Bayesian posterior and average individual squid weight at the end of the season. Blue lines: maximum likelihood and 95% confidence interval. Note correspondence to Figure 7.

The MCMC distribution of the Bayesian posterior multiplied by the GAM fit of average individual squid weight (Figure A1-south) gave the likelihood distribution of *D. gahi* biomass on day 280 (October 6th) shown in Figure 6-right, with maximum likelihood and 95% confidence interval of:

$$B_{S\ day\ 280} = 4{,}936\ t \sim 95\%\ CI\ [3{,}361 - 8{,}432]\ t \qquad \textbf{(8-S)}$$

On the first day of the season estimated *D. gahi* biomass south was 26,287 t ~ 95% CI [22,636 – 34,266] t (Figure 7); considerably lower than the pre-season estimate of 39,177 t [25,608 – 76,321] (Winter et al. 2020). The depletion model performed poorly at embracing the high catches of the first seven days (Figure A2-S), suggesting that the early high concentrations of *D. gahi* exited from the system for causes other than either fishing or natural mortality. In the previous second season, a putative emigration was explicitly modelled (Winter 2019b). To do so was not judged necessary for the current season, in the absence of an observed event that would have triggered it. Underperformance on high catches, while not desirable, will err towards conservatism of the biomass estimate and therefore minimize risk to the stock. The second immigration on day 250 was modest, but still increased biomass to a level that was significantly higher than biomass at season end, by the rule that a straight line could be drawn through the plot (Figure 7) without intersecting the 95% confidence intervals (Swartzman et al. 1992).

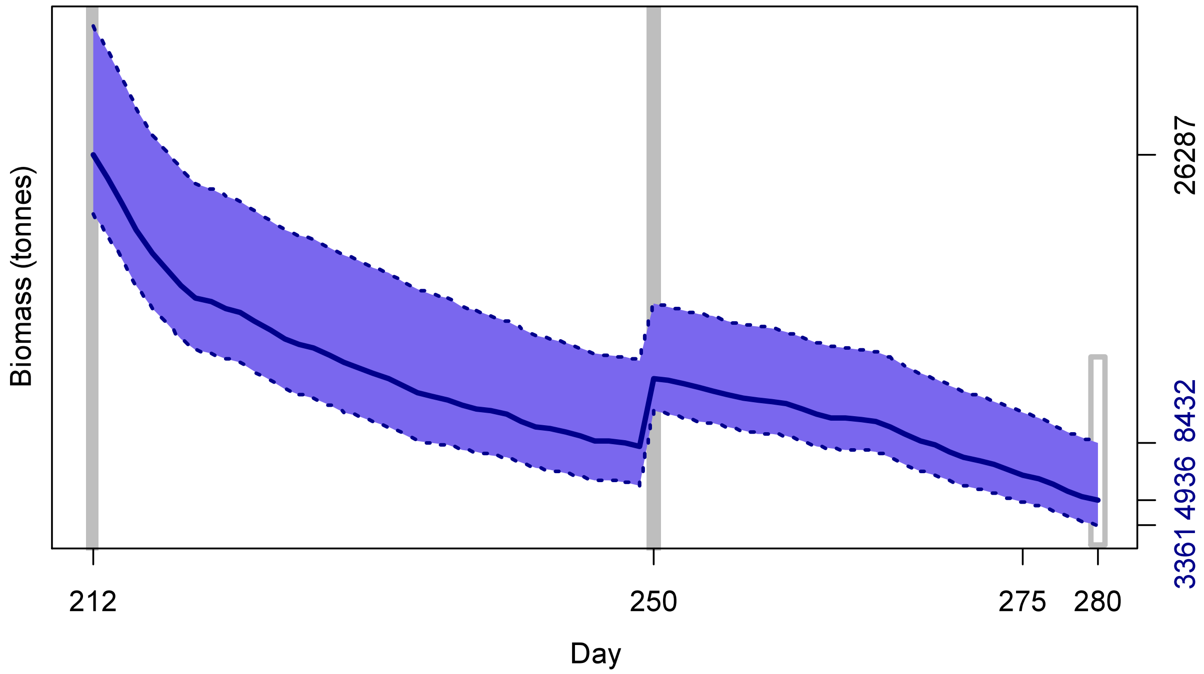

Figure 7. South sub-area. *D. gahi* biomass time series estimated from Bayesian posterior of the depletion model ± 95% confidence intervals. Grey bars indicate the start of in-season depletions south; days 212 and 250. Note that the biomass 'footprint' on day 280 (October 6th) corresponds to the right-side plot of Figure 7.

North

In the north sub-area, the in-season depletion model optimized on a high catchability q ($_{\text{depletion}}\ q_{\text{N}}$ = 3.674 × 10^{-3}; off the scale on Figure 8-left, and Equation **A6-N**) and correspondingly low catch number estimates, compared to the pre-season prior ($_{\text{prior}}\ q_{\text{N}}$ = 1.542 × 10^{-3}; Figure 8-left, and Equation **A4-N**). The resulting maximum likelihood posterior ($_{\text{Bayesian}}\ q_{\text{N}}$ = 1.778 × 10^{-3}; Figure 8-left, and Equation **A9-N**) was more closely determined by the prior, despite higher modelling weight of the in-season depletion (0.648, **A5-N**) than the prior (0.382, **A8-N**).

The MCMC distribution of the Bayesian posterior multiplied by the generalized additive model (GAM) fit of average individual squid weight (Figure A1-north) gave the likelihood distribution of *D. gahi* biomass on day 280 (October 6th) shown in Figure 8-right, with maximum likelihood and 95% confidence interval of:

$B_{\text{N day 280}}$ = 7,011 t ~ 95% CI [2,200 – 12,625] t **(8-N)**

On the first day of the season estimated *D. gahi* biomass north was 19,759 t ~ 95% CI [14,762 – 33,601] t (Figure 9). As in the south, this in-season biomass estimate was considerably lower than the pre-season estimate of 53,017 t [31,516 – 86,476] (Winter et al. 2020), and demonstrated by poor fit of the depletion model to high catches (Figure A2-N). The highest biomass estimate of the season occurred with the second immigration on day 232, reaching 21,160 t [18,279 – 29,413], and thereafter declining steadily (Figure 9).

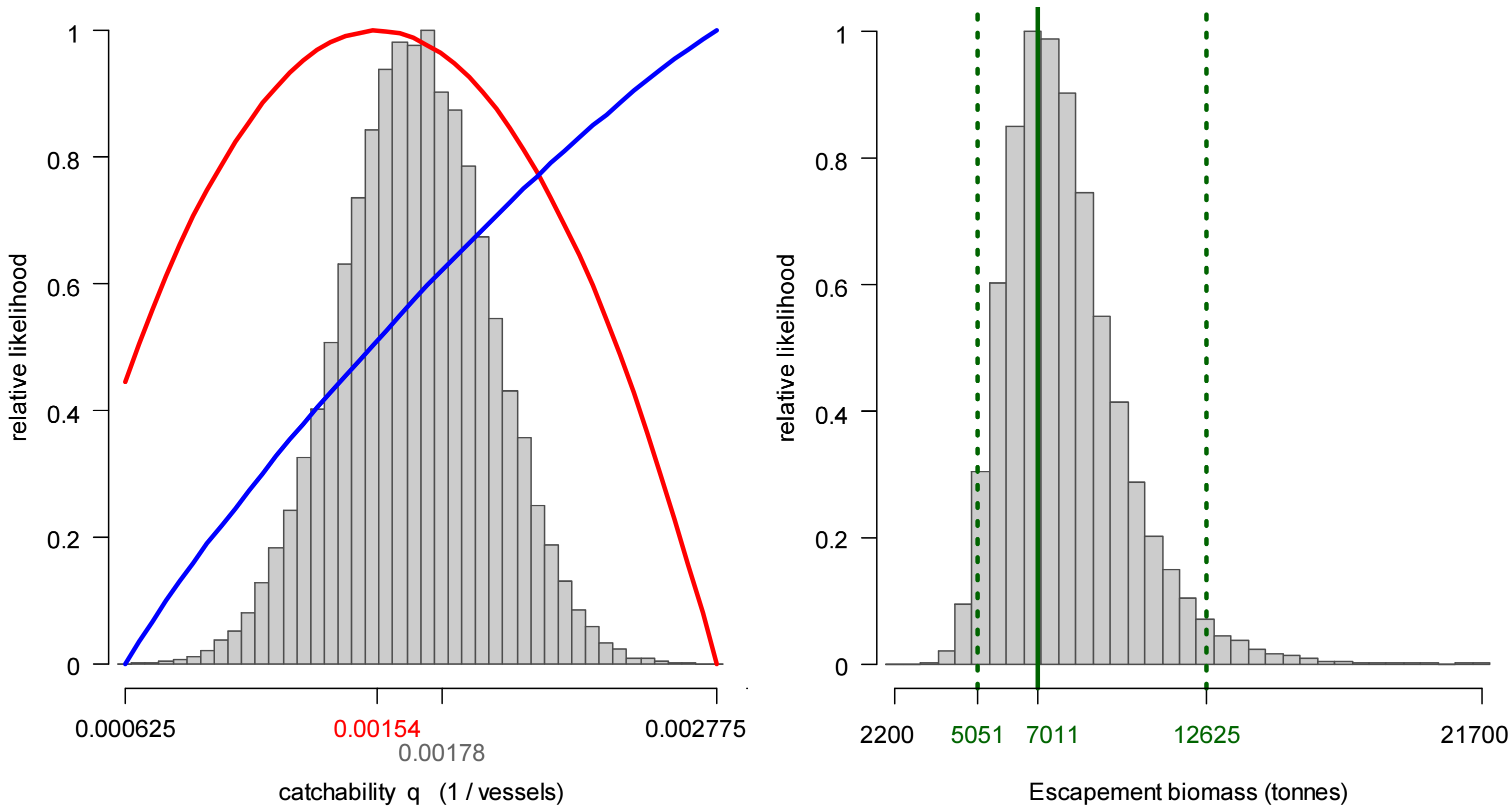

Figure 8. North sub-area. Left: Likelihood distributions for *D. gahi* catchability. Red line: prior model (pre-season survey data), blue line: in-season depletion model, grey bars: combined Bayesian model posterior. Right: Likelihood distribution (grey bars) of escapement biomass, from Bayesian posterior and average individual squid weight at the end of the season. Green lines: maximum likelihood and 95% confidence interval. Note the correspondence to Figure 9.

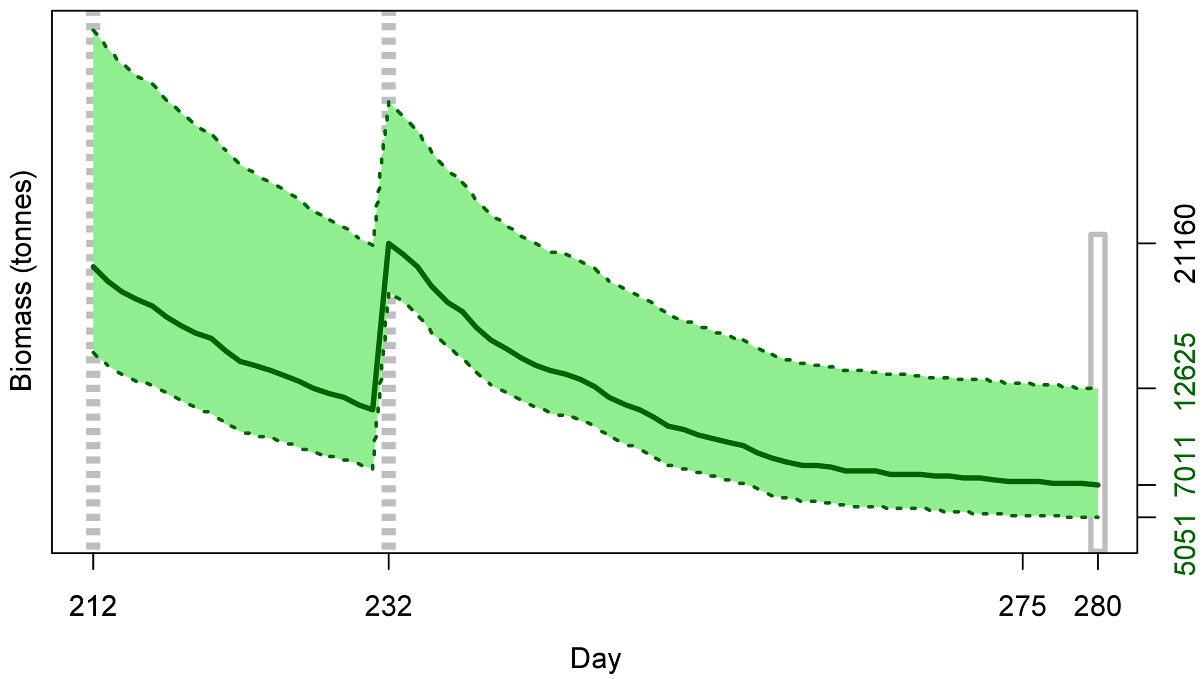

Figure 9 [previous page]. North sub-area. *D. gahi* biomass time series estimated from Bayesian posterior of the depletion model ± 95% confidence intervals. Broken grey bars indicate the start of in-season depletions north; days 212 and 232. Note that the biomass 'footprint' on day 280 (October 6th) corresponds to the right-side plot of Figure 8.

Immigration

Doryteuthis gahi immigration during the season was inferred on each day by how many more squid were estimated present than the day before, minus the number caught and the number expected to have died naturally:

$$_{\text{Immigration}}N_{\text{day } i} = N_{\text{day } i} - (N_{\text{day } i\text{-}1} - C_{\text{day } i\text{-}1} - M_{\text{day } i\text{-}1})$$

where $N_{\text{day } i\text{-}1}$ are optimized in the depletion models, $C_{\text{day } i\text{-}1}$ calculated as in Equation **3**, and $M_{\text{day } i\text{-}1}$ is:

$$M_{\text{day } i\text{-}1} = (N_{\text{day } i\text{-}1} - C_{\text{day } i\text{-}1}) \times (1 - e^{-M})$$

Immigration biomass per day was then calculated as the immigration number per day multiplied by predicted average individual weight from the GAM:

$$_{\text{Immigration}}B_{\text{day } i} = {}_{\text{Immigration}}N_{\text{day } i} \times {}_{\text{GAM}}Wt_{\text{day } i}$$

All numbers N are themselves derived from the daily average individual weights, therefore the estimation automatically factors in that those squid immigrating on a given day would likely be smaller than average (because younger). Confidence intervals of the immigration estimates were calculated by applying the above algorithms to the MCMC iterations of the depletion models. Resulting total biomasses of *D. gahi* immigration north and south, up to season end (day 280), were:

$$_{\text{Immigration}}B_{\text{S season}} = 3{,}454 \text{ t} \sim 95\% \text{ CI } [341 \text{ to } 6{,}814] \text{ t} \quad \textbf{(9-S)}$$

$$_{\text{Immigration}}B_{\text{N season}} = 7{,}568 \text{ t} \sim 95\% \text{ CI } [1{,}925 \text{ to } 12{,}827] \text{ t} \quad \textbf{(9-N)}$$

Total immigration with semi-randomized addition of the confidence intervals was:

$$_{\text{Immigration}}B_{\text{Total season}} = 11{,}022 \text{ t} \sim 95\% \text{ CI } [3{,}405 \text{ to } 18{,}511] \text{ t} \quad \textbf{(9-T)}$$

In the south sub-area, the in-season peak on day 250 accounted for approximately 69.8% of in-season immigration (start day 212 was de facto not an in-season immigration). The minor 'bumps' throughout the season, visible on Figure 7, accounted for the rest. In the north sub-area, the in-season peak on day 232 accounted for approximately 95.4% of in-season immigration, consistent with the prominence of this peak on Figure 9.

Escapement biomass

Total escapement biomass was defined as the aggregate biomass of *D. gahi* at the end of day 280 (October 6th) for south and north sub-areas combined (Equations **8-S** and **8-N**). Depletion models are calculated on the inference that all fishing and natural mortality are gathered at mid-day, thus a half day of mortality ($e^{-M/2}$) was added to correspond to the closure of the fishery at 23:59 (mid-night) on October 6th for the final remaining vessel: Equation **10**.

$$B_{\text{Total day 280}} = (B_{\text{S day 280}} + B_{\text{N day 280}}) \times e^{-M/2}$$
$$= 11{,}947 \text{ t} \times 0.99336$$
$$= 11{,}867 \text{ t} \sim 95\% \text{ CI } [8{,}855 - 19{,}744] \text{ t} \qquad \textbf{(10)}$$

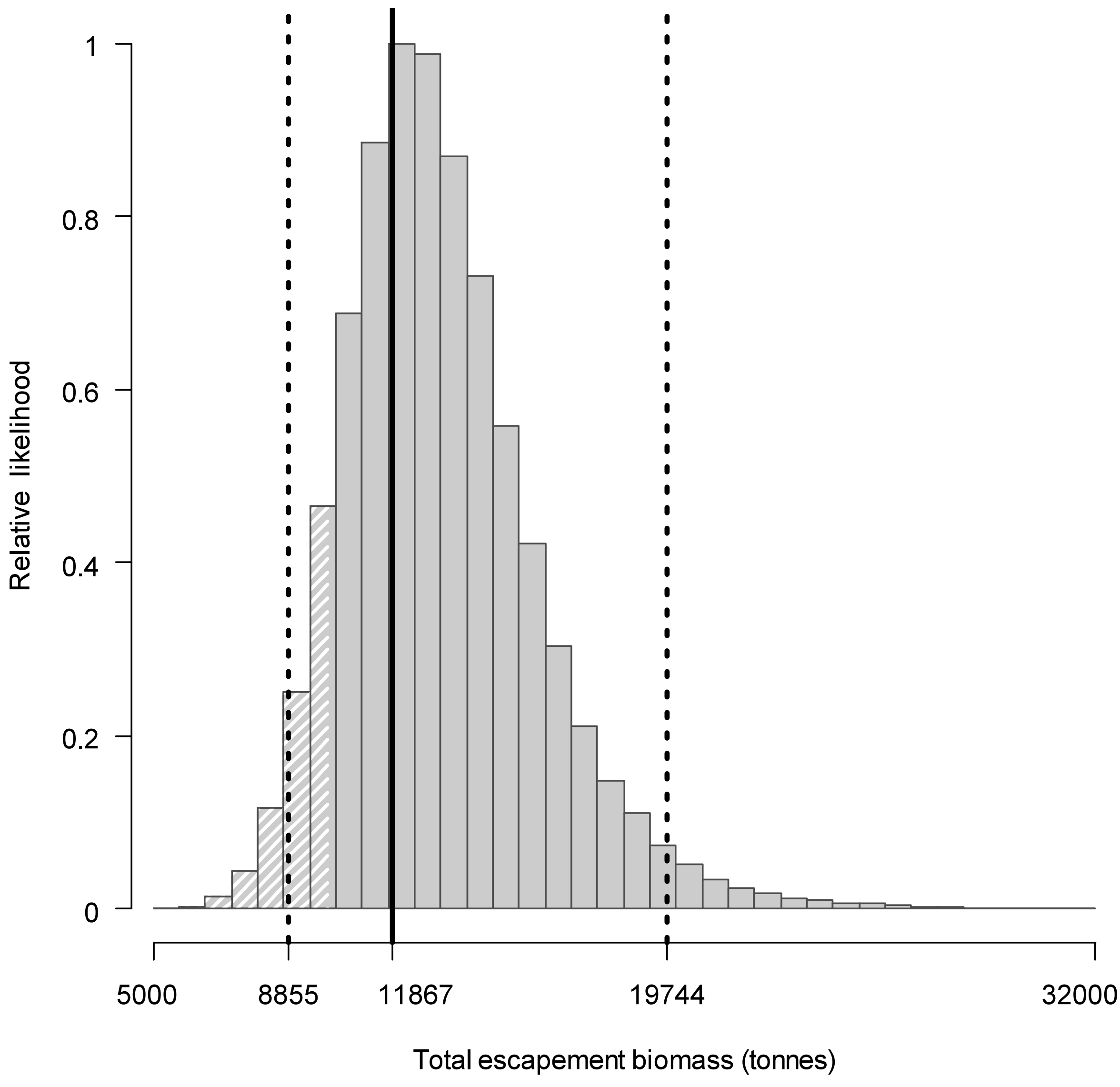

Figure 10. Likelihood distribution with 95% confidence intervals of total *D. gahi* escapement biomass at the season end (October 6th). White shading lines: portion of the distribution < 10,000 tonnes; equal to 8.83% of the whole distribution.

South and north biomass season time series were overall correlated with each other at R = +0.679). Semi-randomized addition of the south and north distributions gave the aggregate likelihood of total escapement biomass shown in Figure 10[d]. The estimated escapement biomass of 11,867 t was the lowest for a season not closed by emergency order since first season 2011 (Winter 2011). The risk of the fishery in the current season, defined as the proportion of the total escapement biomass distribution below the conservation limit of 10,000 tonnes (Agnew et al. 2002, Barton 2002), was calculated as 8.83%.

Fishery bycatch

All except three of the 993 second season vessel-days (Table 1) reported *D. gahi* squid as their primary catch. The exceptions were one vessel-day in the northern part of the Loligo Box that reported 68.8% hoki (*Macruronus magellanicus*) vs. 30.2% *D. gahi*, and two vessel-days in the south that reported 57.3% and 48.7% red cod (*Salilota australis*) vs. 42.0% and 43.7% *D. gahi*. The proportion of season total catch represented by *D. gahi* (29759086/30351955 = 0.9805; Table A1) is the second-highest for a second season since 1992; after last year. Highest bycatches in second season 2020 were common hake *Merluccius hubbsi*, with 256 tonnes from 765 vessel-days, rock cod *Patagonotothen ramsayi* (145 t, 926 v-days), red cod (92 t, 207 v-days), hoki (29 t, 25 v-days), frogmouth *Cottoperca gobio* (17 t, 670 v-days), skate Rajiformes (14 t, 6855 v-days), scallops probably *Zygochlamys* (12 t, 365 v-days), and grenadier *Macrourus* (6 t, 125 v-days). Relative distributions by grid of these bycatches are shown in Figure 11; the complete list of all catches by species is in Table A1.

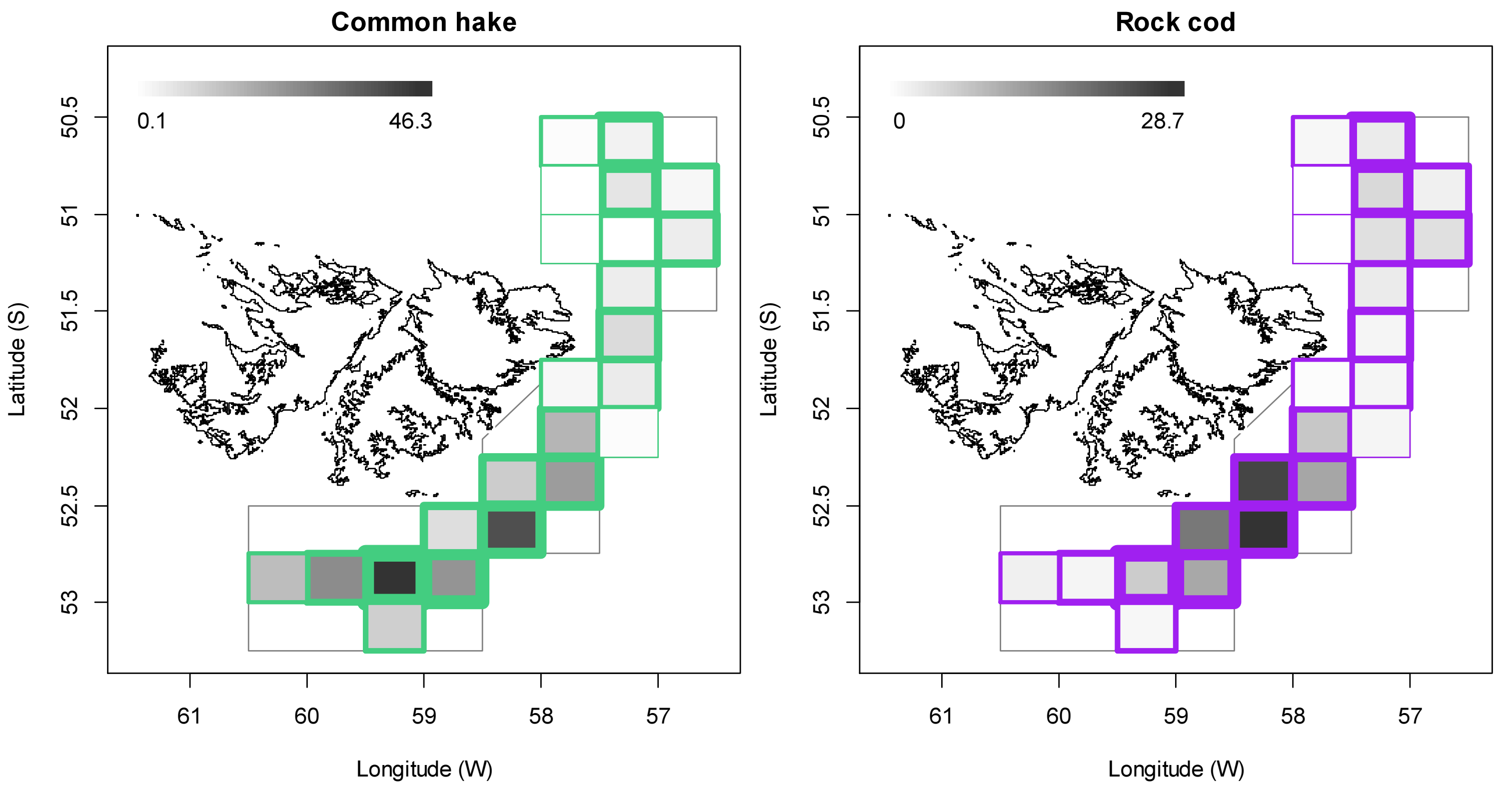

[d] Figure 10 is censored to curtail its right-skewness. The maximum distributional estimates from semi-randomized addition were >42,000 tonnes.

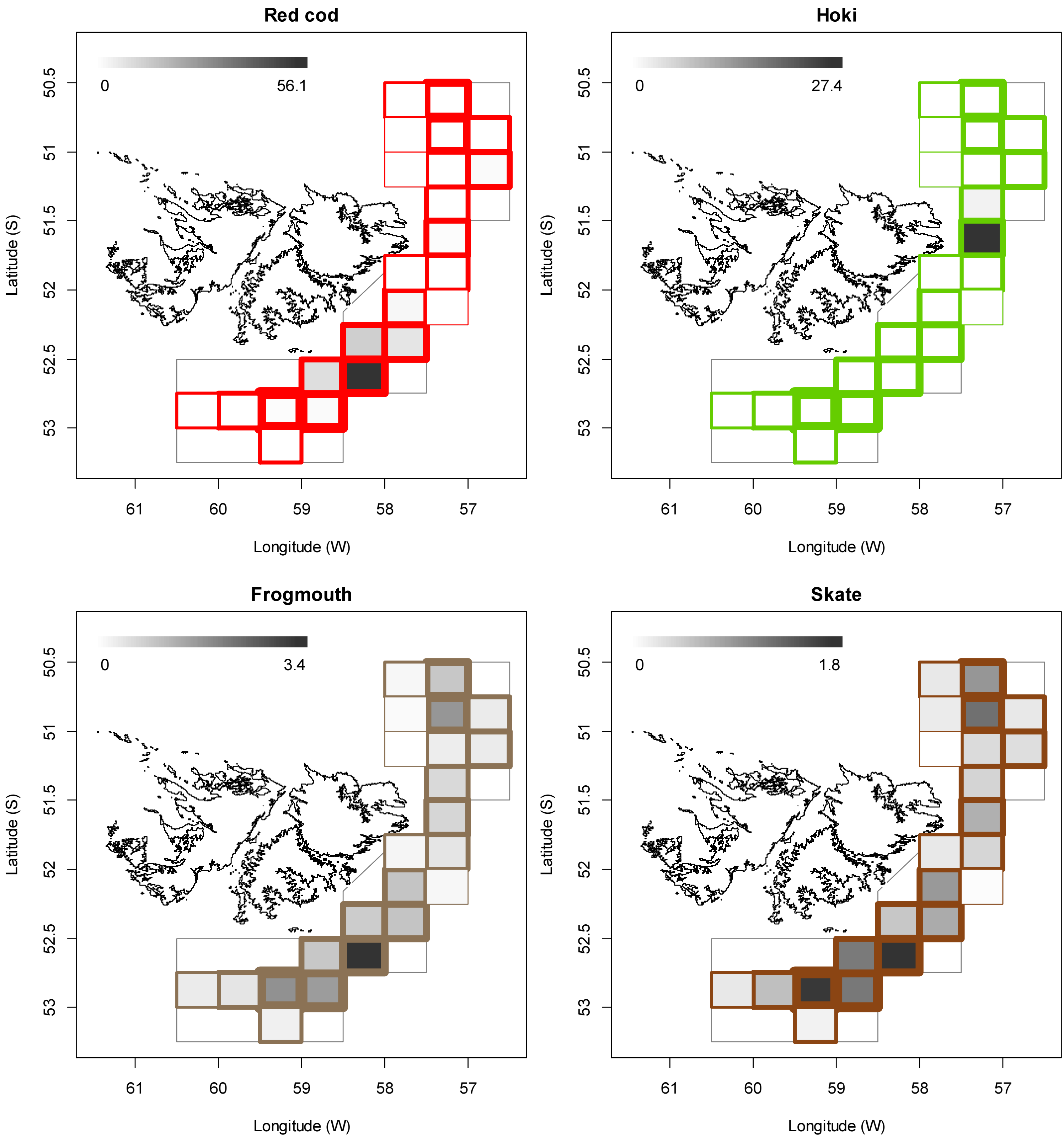
Red cod
0
56.1
Latitude (S)
Longitude (W)
Hoki
0
27.4
Latitude (S)
Longitude (W)
Frogmouth
0
3.4
Latitude (S)
Longitude (W)
Skate
0
1.8
Latitude (S)
Longitude (W)

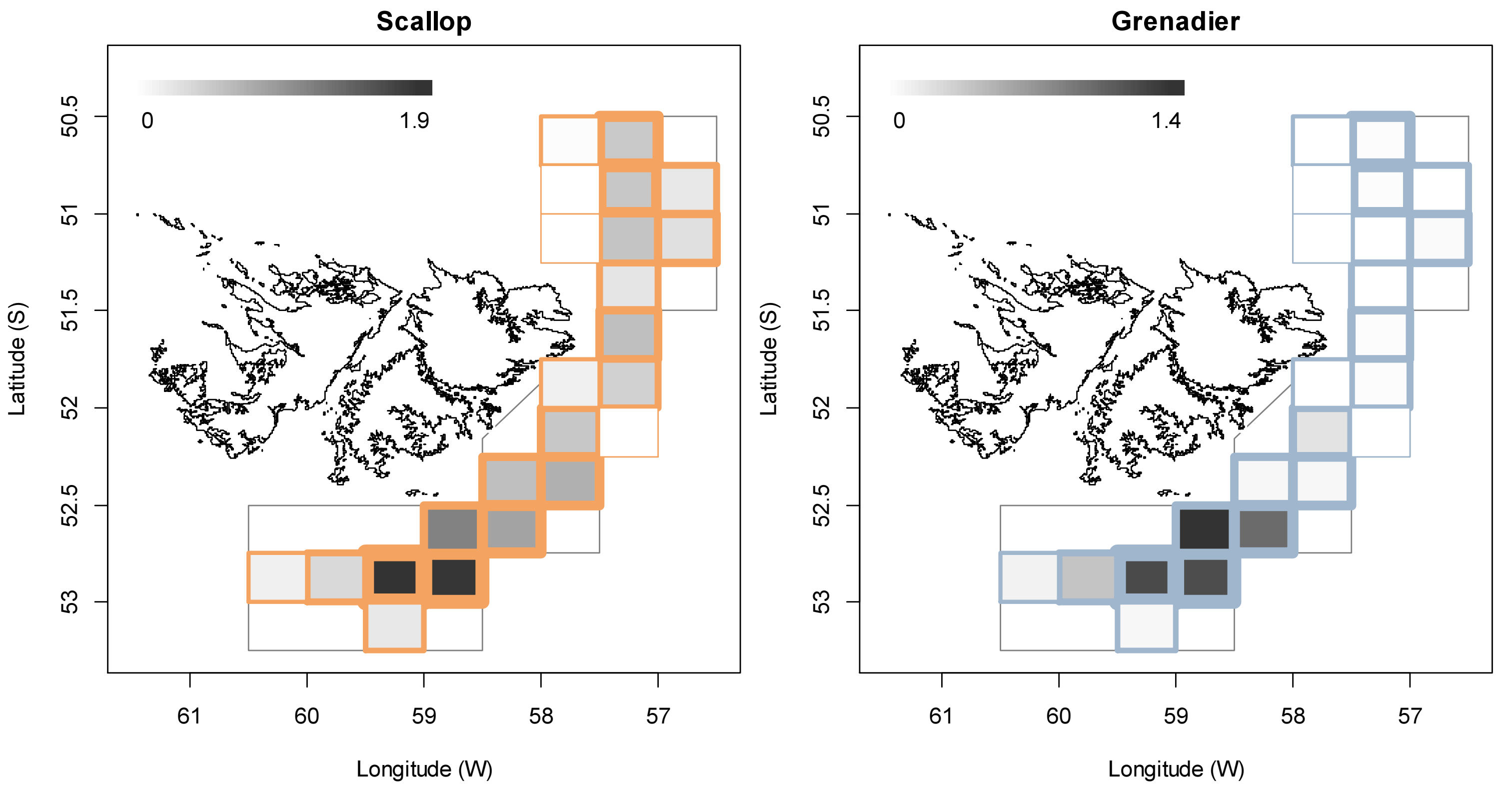

Figure 11. Distributions of the eight principal bycatches during 2nd season 2020, by noon position grids. Thickness of grid lines is proportional to the number of vessel-days (2 to 159 per grid; 23 different grids were occupied). Grey-scale is proportional to the bycatch biomass; maximum (tonnes) indicated on each plot.

Trawl area coverage

The impact of bottom trawling on seafloor habitat has been a matter of concern in commercial fisheries (Kaiser et al. 2002; 2006), whereby the potential severity of impact relates to spatial and temporal extents of trawling (Piet and Hintzen 2012, Gerritsen et al. 2013). For the *D. gahi* fishery, available catch, effort, and positional data are used to summarize the estimated 'ground' area coverage occupied during the season of trawling.

The procedure for summarizing trawl area coverage is described in the Appendix of the second season 2019 report (Winter 2019b). In first season 2020 50% of total *D. gahi* catch was taken from 2.8% of the total area of the Loligo Box, corresponding approximately[e] to the aggregate of grounds trawled ≥7.6 times. 90% of total *D. gahi* catch was taken from 11.5% of the total area of the Loligo Box, corresponding approximately to the aggregate of grounds trawled ≥2.6 times. 100% of total *D. gahi* catch over the season was taken from 17.6% of the total area of the Loligo Box, obviously corresponding to the aggregate of all grounds trawled at least once (Figure 12 - left). The 17.6% total trawl area coverage is the highest among the five seasons that have been given this analysis so far. Averaged by 5 × 5 km grid (Figure 12 - right), 11 grids (out of 1383) had coverage of 10 or more (that is to say, every patch of ground within that 5 × 5 km was on average trawled over 10 times or more). Forty-six grids had coverage of 5 or more, and 150 grids had coverage of 2 or more.

[e] However, not exactly. There is an expected strong correlation between the density of *D. gahi* catch taken from area units and how often these area units were trawled, but the correlation is not perfectly monotonic.

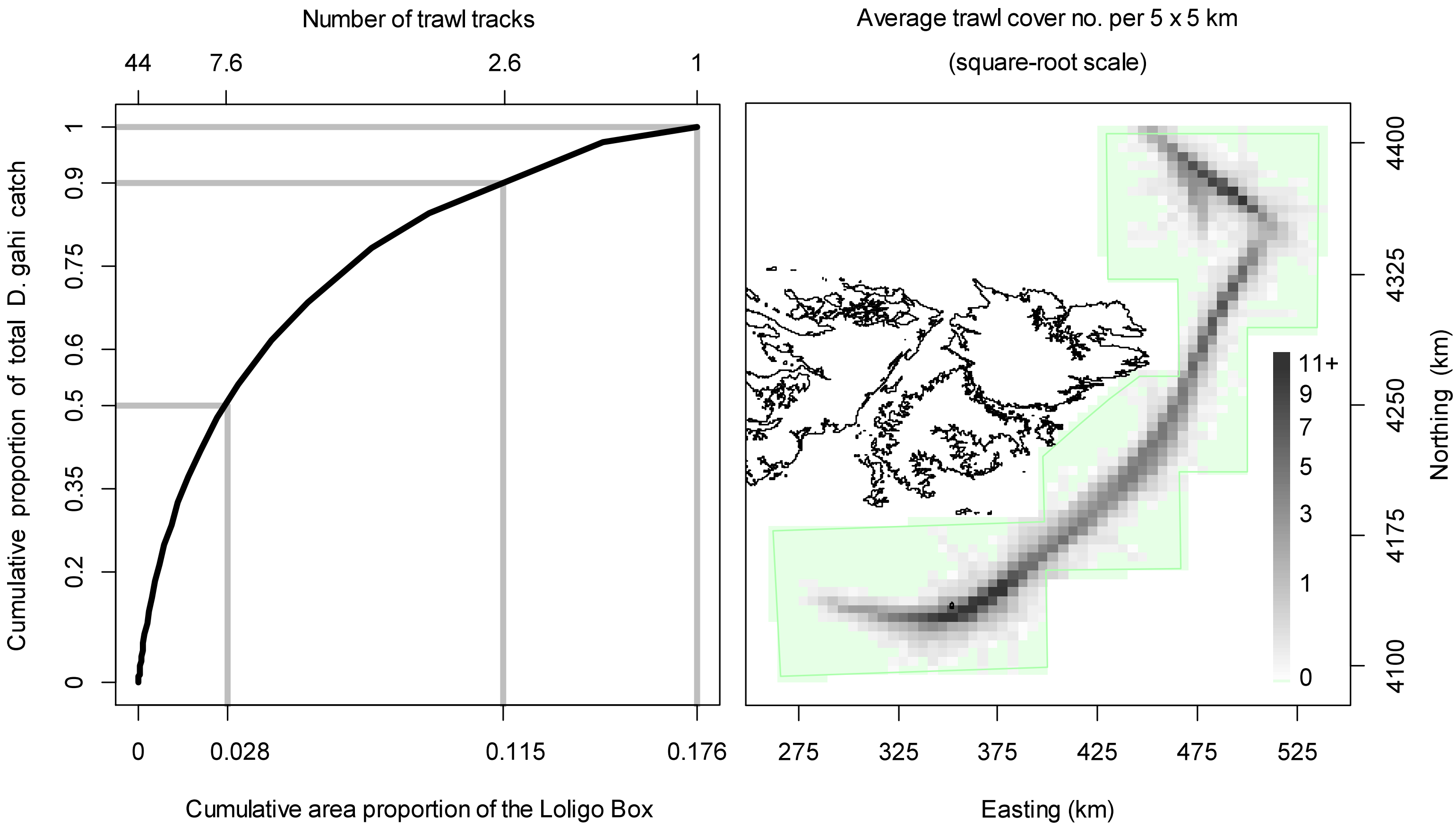

Figure 12. Left: cumulative *D. gahi* catch of 2nd season 2020, vs. cumulative area proportion of the Loligo Box the catch was taken from. The maximum number of times that any single area unit was trawled was 44, and catch cumulation by reverse density corresponded approximately to the trawl multiples shown on the top x-axis. Right: trawl cover averaged by 5 × 5 km grid; green area represents zero trawling.

References

Agnew, D.J., Baranowski, R., Beddington, J.R., des Clers, S., Nolan, C.P. 1998. Approaches to assessing stocks of *Loligo gahi* around the Falkland Islands. Fisheries Research 35: 155-169.

Agnew, D. J., Beddington, J. R., and Hill, S. 2002. The potential use of environmental information to manage squid stocks. Canadian Journal of Fisheries and Aquatic Sciences, 59: 1851–1857.

Arkhipkin, A. 1993. Statolith microstructure and maximum age of *Loligo gahi* (Myopsida: Loliginidae) on the Patagonian Shelf. Journal of the Marine Biological Association of the UK 73: 979-982.

Arkhipkin, A.I., Middleton, D.A.J. 2002. Sexual segregation in ontogenetic migrations by the squid *Loligo gahi* around the Falkland Islands. Bulletin of Marine Science 71: 109-127.

Arkhipkin, A.I., Middleton, D.A.J., Barton, J. 2008. Management and conservation of a short-lived fishery resource: *Loligo gahi* around the Falkland Islands. American Fisheries Society Symposium 49: 1243-1252.

Arkhipkin, A.I., Hendrickson, L.C., Payá, I., Pierce, G.J., Roa-Ureta, R.H., Robin, J.-P., Winter, A. 2020. Stock assessment and management of cephalopods: advances and challenges for short-lived fishery resources. ICES Journal of Marine Science, doi:10.1093/icesjms/fsaa038.

Barton, J. 2002. Fisheries and fisheries management in Falkland Islands Conservation Zones. Aquatic Conservation: Marine and Freshwater Ecosystems 12: 127–135.

Brewin, J. 2020. Observer Report 1273. Technical Document, FIG Fisheries Department. 37 p.

Brooks, S.P., Gelman, A. 1998. General methods for monitoring convergence of iterative simulations. Journal of computational and graphical statistics 7:434-455.

DeLury, D.B. 1947. On the estimation of biological populations. Biometrics 3: 145-167.

Evans, D. 2020. Observer Report 1271. Technical Document, FIG Fisheries Department. 31 p.

FIFD / LPG 2017. Loligo vessel substitution and other rules. Memorandum of understanding between the Falkland Islands Fisheries Department and the Loligo Producers Group, March 2017.

Gamerman, D., Lopes, H.F. 2006. Markov Chain Monte Carlo. Stochastic simulation for Bayesian inference. 2nd edition. Chapman & Hall/CRC.

Gerritsen, H.D., Minto, C., Lordan, C. 2013. How much of the seabed is impacted by mobile fishing gear? Absolute estimates from Vessel Monitoring System (VMS) point data. ICES Journal of Marine Science 70: 523-531.

Hoenig, J.M. 1983. Empirical use of longevity data to estimate mortality rates. Fishery Bulletin 82: 898-903

Iriarte, V., Arkhipkin, A., Blake, D. 2020. Implementation of exclusion devices to mitigate seal (*Arctocephalus australis*, *Otaria flavescens*) incidental mortalities during bottom-trawling in the Falkland Islands (Southwest Atlantic). Fisheries Research 227: 105537, 12 p.

Kaiser, M.J., Collie, J.S., Hall, S.J., Jennings, S., Poiner, I.R. 2002. Modification of marine habitats by trawling activities: prognosis and solutions. Fish and Fisheries 3: 114-136.

Kaiser, M.J., Clarke, K.R., Hinz, H., Austen, M.C.V., Somerfield, P.J., Karakassis, I. 2006. Global analysis of response and recovery of benthic biota to fishing. Marine Ecology Progress Series 311: 1-14.

Magnusson, A., Punt, A., Hilborn, R. 2013. Measuring uncertainty in fisheries stock assessment: the delta method, bootstrap, and MCMC. Fish and Fisheries 14: 325-342.

Matošević, N. 2020a. Observer Report 1270. Technical Document, FIG Fisheries Department. 25 p.

Matošević, N. 2020b. Observer Report 1274. Technical Document, FIG Fisheries Department. 22 p.

Matošević, N. 2020c. Observer Report 1276. Technical Document, FIG Fisheries Department. 28 p.

Nash, J.C., Varadhan, R. 2011. optimx: A replacement and extension of the optim() function. R package version 2011-2.27. http://CRAN.R-project.org/package=optimx

Patterson, K.R. 1988. Life history of Patagonian squid *Loligo gahi* and growth parameter estimates using least-squares fits to linear and von Bertalanffy models. Marine Ecology Progress Series 47: 65-74.

Payá, I. 2010. Fishery Report. *Loligo gahi*, Second Season 2009. Fishery statistics, biological trends, stock assessment and risk analysis. Technical Document, Falkland Islands Fisheries Dept. 54 p.

Pierce, G.J., Guerra, A. 1994. Stock assessment methods used for cephalopod fisheries. Fisheries Research 21: 255–285.

Piet, G.J., Hintzen, N.T. 2012. Indicators of fishing pressure and seafloor integrity. ICES Journal of Marine Science 69: 1850-1858.

Powell, D.M. 1998. Patterns and processes of sediment sorting in gravel-bed rivers. Progress in Physical Geography 22: 1–32.

Punt, A.E., Hilborn, R. 1997. Fisheries stock assessment and decision analysis: the Bayesian approach. Reviews in Fish Biology and Fisheries 7:35-63.

Roa-Ureta, R. 2012. Modelling in-season pulses of recruitment and hyperstability-hyperdepletion in the *Loligo gahi* fishery around the Falkland Islands with generalized depletion models. ICES Journal of Marine Science 69: 1403–1415.

Roa-Ureta, R., Arkhipkin, A.I. 2007. Short-term stock assessment of *Loligo gahi* at the Falkland Islands: sequential use of stochastic biomass projection and stock depletion models. ICES Journal of Marine Science 64: 3-17.

Rosenberg, A.A., Kirkwood, G.P., Crombie, J.A., Beddington, J.R. 1990. The assessment of stocks of annual squid species. Fisheries Research 8: 335-350.

Shaw, P.W., Arkhipkin, A.I., Adcock, G.J., Burnett, W.J., Carvalho, G.R., Scherbich, J.N., Villegas, P.A. 2004. DNA markers indicate that distinct spawning cohorts and aggregations of Patagonian squid, *Loligo gahi*, do not represent genetically discrete subpopulations. Marine Biology, 144: 961-970.

Swartzman, G., Huang, C., Kaluzny, S. 1992. Spatial analysis of Bering Sea groundfish survey data using generalized additive models. Canadian Journal of Fisheries and Aquatic Sciences 49: 1366-1378.

Winter, A. 2011. *Loligo gahi* stock assessment, First season 2011. Technical Document, Falkland Islands Fisheries Department. 23 p.

Winter, A. 2014. *Loligo* stock assessment, second season 2014. Technical Document, Falkland Islands Fisheries Department. 30 p.

Winter, A. 2017. Stock assessment – *Doryteuthis gahi* 2nd season 2017. Technical Document, Falkland Islands Fisheries Department. 37 p.

Winter, A. 2019a. Stock assessment –Falkland calamari *Doryteuthis gahi* 1st season 2019. Technical Document, Falkland Islands Fisheries Department. 37 p.

Winter, A. 2019b. Stock assessment –Falkland calamari *Doryteuthis gahi* 2nd season 2019. Technical Document, Falkland Islands Fisheries Department. 36 p.

Winter, A., Arkhipkin, A. 2015. Environmental impacts on recruitment migrations of Patagonian longfin squid (*Doryteuthis gahi*) in the Falkland Islands with reference to stock assessment. Fisheries Research 172: 85-95.

Winter, A., Ramos, J.E., Shcherbich, Z., Tutjavi, V., Matošević, N. 2020. Falkland calamari (*Doryteuthis gahi*) stock assessment survey, 2nd season 2020. Technical Document, Falkland Islands Fisheries Department. 17 p.

Appendix
***Doryteuthis gahi* individual weights**

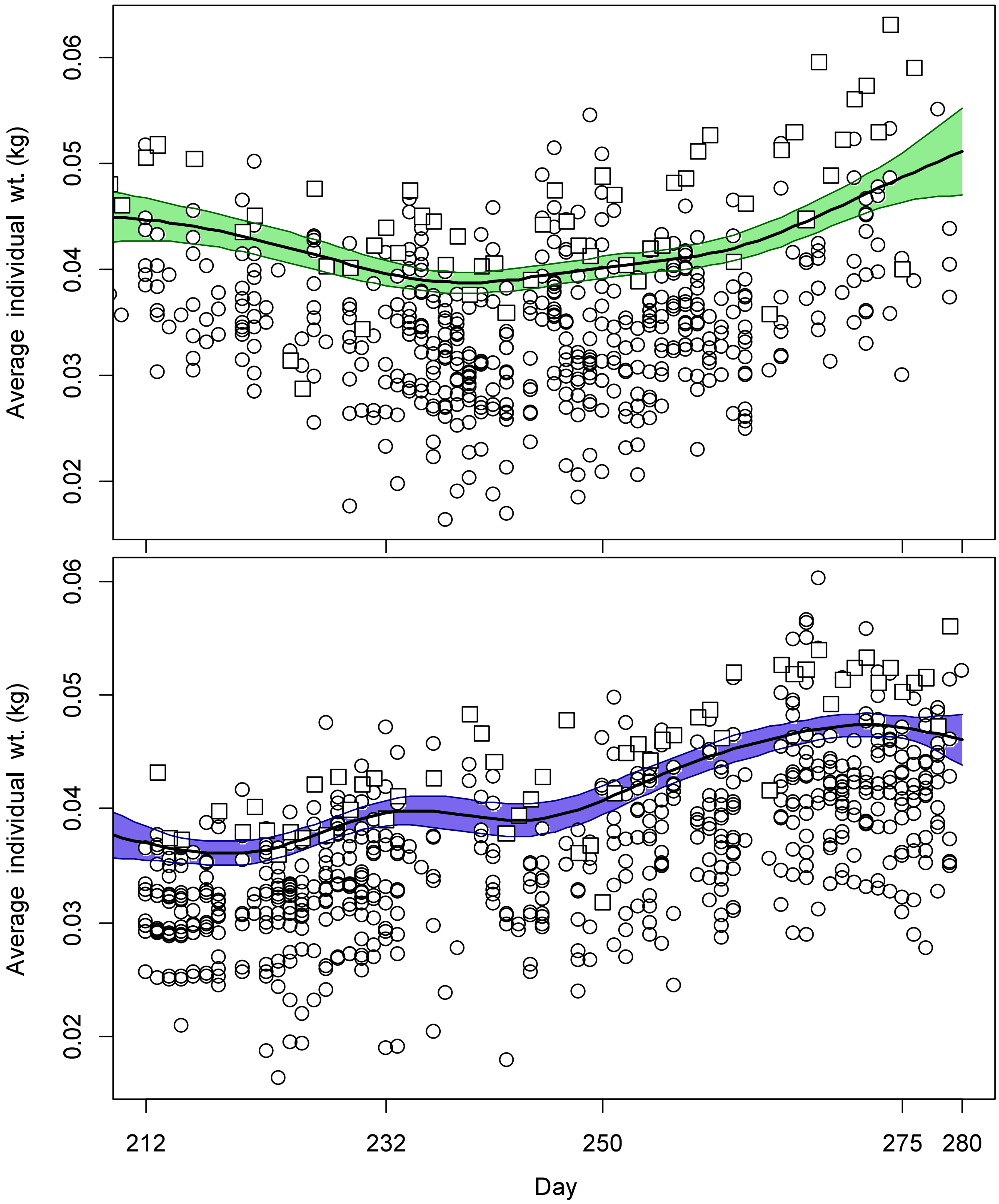

Figure A1. North (top) and south (bottom) sub-area daily average individual *D. gahi* weights from commercial size categories per vessel (circles) and observer measurements (squares). GAMs of the daily trends ± 95% confidence intervals (centre lines and colour under-shading).

To smooth fluctuations, GAM trends were calculated of daily average individual weights. North and south sub-areas were calculated separately. For continuity, GAMs were calculated using all pre-season survey and in-season data contiguously. North and south GAMs were first calculated separately on the commercial and observer data. Commercial data GAMs were taken as the baseline trends, and calibrated to observer data GAMs in proportion to the correlation between commercial data and observer data GAMs. For example, if the season average individual weight estimate from commercial data was 0.052 kg, the season average individual weight estimate from observer data was 0.060 kg, and the coefficient of determination (R^2) between commercial and observer GAM trends was 86%, then the resulting trend of daily average individual weights was calculated as the commercial data GAM values + (0.060 – 0.052) × 0.86. This way, both the greater day-to-day consistency of the commercial data trends, and the greater point value accuracy of the observer data are represented in the calculations. GAM plots of the north and south sub-areas are in Figure A1.

Prior estimates and CV

The pre-season survey had estimated *D. gahi* biomasses of 53,017 t north of 52° S and 39,177 t south of 52° S (Winter et al. 2020). Hierarchical bootstrapping of the inverse distance weighting algorithm obtained coefficients of variation (CV) equal to 24.6% of the survey biomass distribution north and 27.9% south. From modelled survey catchability, Payá (2010) had estimated average net escapement of up to 22%, which was added to the CV:

$$39{,}177 \pm (.279 + .22) = 39{,}177 \pm 49.9\% = 39{,}177 \pm 19{,}544 \text{ t} \qquad \textbf{(A1-S)}$$

$$53{,}017 \pm (.246 + .22) = 53{,}017 \pm 46.6\% = 53{,}017 \pm 24{,}700 \text{ t} \qquad \textbf{(A1-N)}$$

The 22% escapement was added as a linear increase in the variability, but was not used to reduce the total estimate, because squid that escape one trawl are likely to be part of the biomass concentration that is available to the next trawl.

D. gahi numbers at the end of the survey were estimated as the survey biomasses divided by the GAM-predicted individual weight averages for the survey: 0.0388 kg south, 0.0449 kg north (Figure A1), 0.0407 kg combined. Average coefficients of variation (CV) of the GAM over the duration of the pre-season survey were 3.7% south, 3.5% north. CV of the length-weight conversion relationship (Equation **7**) were 6.9% south, 7.1% north. Joining these sources of variation with the pre-season survey biomass estimates and individual weight averages (above) gave estimated *D. gahi* numbers at survey end (day 210) of:

$$_{\text{prior}}\text{N}_{\text{S day 210}} = \frac{39{,}177 \times 1000}{0.0388} \pm \sqrt{49.9\%^2 + 3.7\%^2 + 6.9\%^2}$$

$$= 1.009 \times 10^9 \pm 50.5\%$$

$$_{\text{prior}}\text{N}_{\text{N day 210}} = \frac{53{,}017 \times 1000}{0.0449} \pm \sqrt{46.6\%^2 + 3.5\%^2 + 7.1\%^2}$$

$$= 1.182 \times 10^9 \pm 47.3\%$$

Priors were normalized for the combined fishing zone average, to produce better continuity as vessels cross back and forth between north and south:

$$_{\text{nprior}}\text{N}_{\text{S day 210}} = \left(\frac{(39{,}177 + 53{,}017) \times 1000}{0.0407}\right) \times \left(\frac{_{\text{prior}}\text{N}_{\text{S day 210}}}{_{\text{prior}}\text{N}_{\text{N day 210}} + {}_{\text{prior}}\text{N}_{\text{S day 210}}}\right)$$

$$= 1.043 \times 10^{9} \pm 50.5\% \qquad \textbf{(A2-S)}$$

$$_{nprior}N_{N\ day\ 210} = \left(\frac{(39{,}177 + 53{,}017) \times 1000}{0.0407}\right) \times \left(\frac{_{prior}N_{N\ day\ 210}}{_{prior}N_{N\ day\ 210} + {}_{prior}N_{S\ day\ 210}}\right)$$

$$= 1.222 \times 10^{9} \pm 47.3\% \qquad \textbf{(A2-N)}$$

The catchability coefficient (q) prior for the south sub-area was taken on day 212, the first day of the season, when 9 vessels fished in the south (Figure 3) and the initial depletion period south started. Abundance on day 212 was discounted for natural mortality over the 2 days since the end of the survey:

$$_{nprior}N_{S\ day\ 212} = {}_{nprior}N_{S\ day\ 210} \times e^{-M\cdot(212-210)} - CNMD_{S\ day\ 212} = 1.016 \times 10^{9} \qquad \textbf{(A3-S)}$$

where $CNMD_{S\ day\ 212} = 0$ as no catches intervened between the end of the survey and the start of commercial season. Thus:

$$_{prior}q_{S} = C(N)_{S\ day\ 212} / ({}_{nprior}N_{S\ day\ 212} \times E_{S\ day\ 212})$$

$$= (C(B)_{S\ day\ 212} / Wt_{S\ day\ 212}) / ({}_{nprior}N_{S\ day\ 212} \times E_{S\ day\ 212})$$

$$= (901.8\ t / 0.036979\ kg) / (1.016 \times 10^{9} \times 9\ \text{vessel-days})$$

$$= 2.667 \times 10^{-3}\ \text{vessels}^{-1} \qquad \textbf{(A4-S)}$$ [f]

CV of the prior was calculated as the sum of variability in $_{nprior}N_{S\ day\ 53}$ (Equation **A2-S**) plus variability in the catches of vessels on start day 55, plus variability of the natural mortality (see Appendix section Natural mortality, below):

$$CV_{prior\ S} =$$

$$\sqrt{50.5\%^2 + \left(\frac{\mathrm{SD}\left(C(B)_{S\ vessels\ day\ 212}\right)}{\mathrm{mean}\left(C(B)_{S\ vessels\ day\ 212}\right)}\right)^2 + (1 - \mathrm{sign}(1 - CV_M) \times \mathrm{abs}(1 - CV_M)^{(212-210)})^2}$$

$$= \sqrt{50.5\%^2 + 14.1\%^2 + 28.5\%^2} \qquad = 59.7\% \qquad \textbf{(A5-S)}$$

The catchability coefficient (q) prior for the north sub-area was also taken on day 212, the first day that fishing was undertaken in the north by 6 vessels (Figure 3) and the initial depletion period north started. Abundance on day 212 was discounted for natural mortality over the 2 days since the end of the survey:

$$_{nprior}N_{N\ day\ 212} = {}_{nprior}N_{N\ day\ 210} \times e^{-M\cdot(212-210)} - CNMD_{N\ day\ 212} = 1.190 \times 10^{9} \qquad \textbf{(A3-N)}$$

where $CNMD_{N\ day\ 212} = 0$ as in the north also no catches intervened between the end of the survey and the start of commercial season. Thus:

[f] On Figure 6-left.

$_{\text{prior}} q_{\text{N}} = C(N)_{\text{N day 212}} / ({}_{\text{nprior}}N_{\text{N day 212}} \times E_{\text{N day 212}})$

$= (C(B)_{\text{N day 212}} / Wt_{\text{N day 212}}) / ({}_{\text{nprior}}N_{\text{N day 212}} \times E_{\text{N day 212}})$

$= (493.0 \text{ t} / 0.044764 \text{ kg}) / (1.190 \times 10^{9} \times 6 \text{ vessel-days})$

$= 1.542 \times 10^{-3} \text{ vessels}^{-1}$ [g] **(A4-N)**

CV of the prior was calculated as the sum of variability in $_{\text{nprior}}N_{\text{N day 53}}$ (Equation **A2-N**) plus variability in the catches of vessels on start day 212, plus variability of the natural mortality (see Appendix section Natural mortality, below):

$CV_{\text{prior N}} =$

$$\sqrt{47.3\%^2 + \left(\frac{\text{SD}\left(C(B)_{\text{N vessels day 212}}\right)}{\text{mean}\left(C(B)_{\text{N vessels day 212}}\right)}\right)^2 + \left(1 - \text{sign}(1 - CV_M) \times \text{abs}(1 - CV_M)^{(212-210)}\right)^2}$$

$$= \sqrt{47.3\%^2 + 34.0\%^2 + 28.5\%^2} = 64.8\% \qquad \textbf{(A5-N)}$$

Depletion model estimates and CV

For the south sub-area, the equivalent of Equation **2** with two N_{day} was optimized on the difference between predicted and actual catches (Equation **3**), resulting in parameters values:

$_{\text{depletion}}N1_{\text{S day 212}} = 1.042 \times 10^{9}$; $_{\text{depletion}}N2_{\text{S day 250}} = 0.070 \times 10^{6}$

$_{\text{depletion}}q_{\text{S}} = 1.360 \times 10^{-3}$ [h] **(A6-S)**

The normalized root-mean-square deviation of predicted vs. actual catches was calculated as the CV of the model:

$$CV_{\text{rmsd S}} = \frac{\sqrt{\sum_{i=1}^{n}\left({}_{\text{predicted}}C(N)_{\text{S day i}} - {}_{\text{actual}}C(N)_{\text{S day i}}\right)^2 / n}}{\text{mean}\left({}_{\text{actual}}C(N)_{\text{S day i}}\right)}$$

$$= 3.781 \times 10^{6} / 6.463 \times 10^{6} = 58.5\% \qquad \textbf{(A7-S)}$$

$CV_{\text{rmsd S}}$ was added to the variability of the GAM-predicted individual weight averages for the season (Figure A1-S); equal to a CV of 1.55% south. CVs of the depletion were then calculated as the sum:

$$CV_{\text{depletion S}} = \sqrt{CV_{\text{rmsd S}}^{\ 2} + CV_{\text{GAM Wt S}}^{\ 2}} = \sqrt{58.5\%^2 + 1.55\%^2}$$

$$= 58.5\% \qquad \textbf{(A8-S)}$$

[g] On Figure 8-left.
[h] On Figure 6-left.

For the north sub-area, the Equation **2** equivalent with two N $_{day}$ was optimized on the difference between predicted and actual catches (Equation **3**), resulting in parameter values:

$$_{depletion}N1_{N\ day\ 212} = 0.232 \times 10^9; \qquad _{depletion}N2_{N\ day\ 232} = 0.257 \times 10^9$$

$$_{depletion}q_{N} = 3.674 \times 10^{-3}\ ^{i} \qquad \textbf{(A6-N)}$$

Root-mean-square deviation of predicted vs. actual catches was calculated as the CV of the model:

$$CV_{rmsd\ N} = \frac{\sqrt{\sum_{i=1}^{n}\left({}_{predicted}C(N)_{N\ day\ i} - {}_{actual}C(N)_{N\ day\ i}\right)^2 / n}}{mean\left({}_{actual}C(N)_{N\ day\ i}\right)}$$

$$= 1.652 \times 10^6 / 4.325 \times 10^6 = 38.2\% \qquad \textbf{(A7-N)}$$

$CV_{rmsd\ N}$ was added to the variability of the GAM-predicted individual weight averages for the season (Figure A1-N); equal to a CV of 1.7% north. CVs of the depletion were then calculated as the sum:

$$CV_{depletion\ N} = \sqrt{CV_{rmsd\ N}^{\ 2} + CV_{GAM\ Wt\ N}^{\ 2}} = \sqrt{38.2\%^2 + 1.7\%^2}$$

$$= 38.2\% \qquad \textbf{(A8-N)}$$

Combined Bayesian models

For the south sub-area, joint optimization of Equations **3** and **4** resulted in parameters values:

$$_{Bayesian}N1_{S\ day\ 212} = 0.711 \times 10^9; \qquad _{Bayesian}N2_{S\ day\ 250} = 0.107 \times 10^9$$

$$_{Bayesian}q_{S} = 2.394 \times 10^{-3}\ ^{j} \qquad \textbf{(A9-S)}$$

For the north sub-area, joint optimization of Equations **3** and **4** resulted in parameters values:

$$_{Bayesian}N1_{N\ day\ 212} = 0.441 \times 10^9; \qquad _{Bayesian}N2_{N\ day\ 232} = 0.253 \times 10^9$$

$$_{Bayesian}q_{N} = 1.778 \times 10^{-3}\ ^{k} \qquad \textbf{(A9-N)}$$

These parameters produced the fit between predicted catches and actual catches shown in Figures A2-S and A2-N.

Figure A2-S [next page top]. Daily catch numbers estimated from actual catch (black points) and predicted from the depletion model (purple line) in the south sub-area.

Figure A2-N [next page bottom]. Daily catch numbers estimated from actual catch (black points) and predicted from the depletion model (green line) in the north sub-area.

---

[i] Off the scale on Figure 8-left.
[j] On Figure 6-left.
[k] On Figure 8-left.

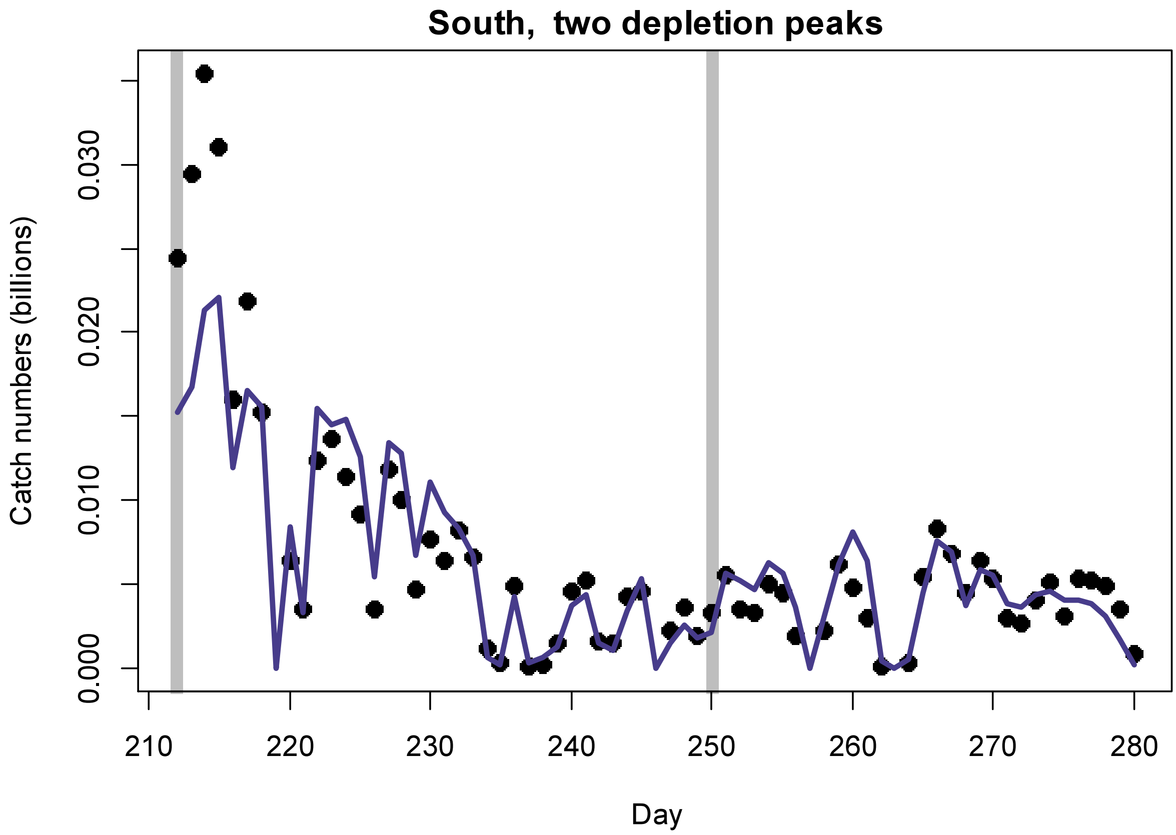
South, two depletion peaks
Catch numbers (billions)
0.000
0.010
0.020
0.030
210
220
230
240
250
260
270
280
Day

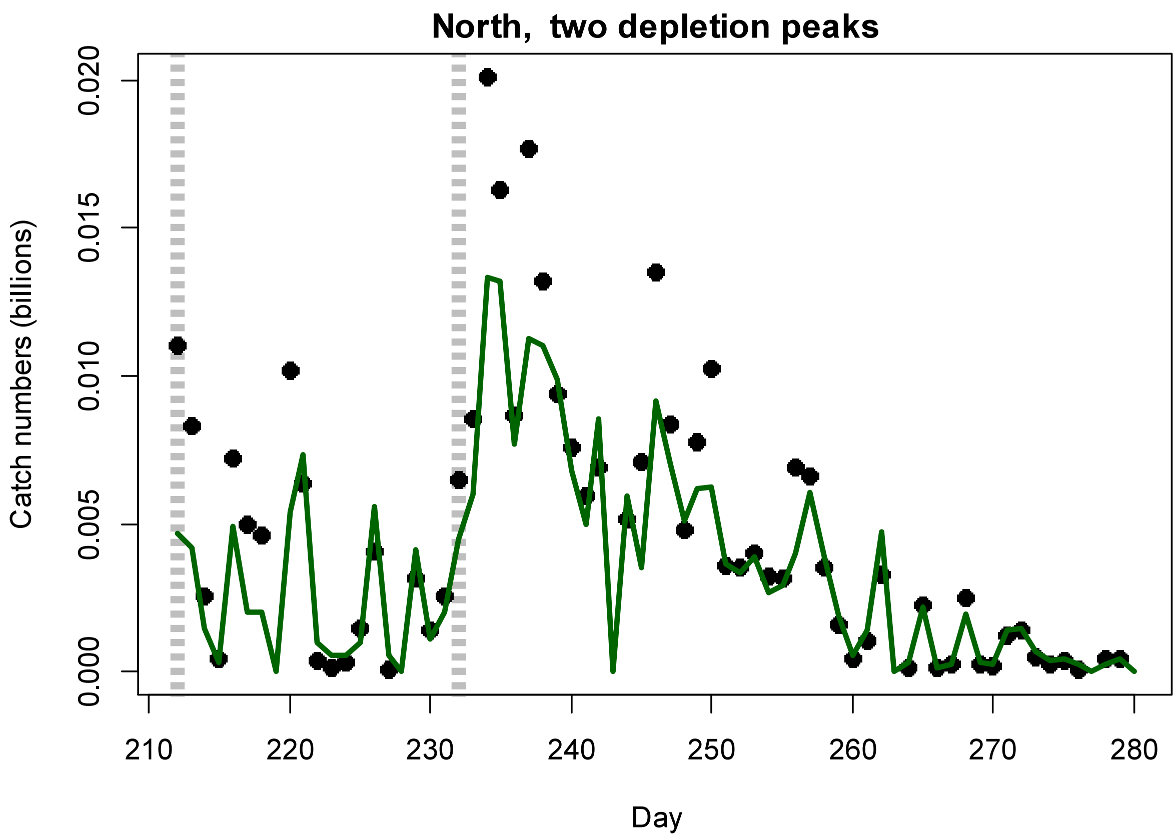
North, two depletion peaks
Catch numbers (billions)
0.000
0.005
0.010
0.015
0.020
210
220
230
240
250
260
270
280
Day

Natural mortality

Natural mortality is parameterized as a constant instantaneous rate M = 0.0133 day^{-1} (Roa-Ureta and Arkhipkin 2007), based on Hoenig's (1983) log mortality vs. log maximum age regression applied to an estimated maximum age of 352 days for *D. gahi*:

$$\log(M) = 1.44 - 0.982 \times \log(\text{age}_{max})$$

$$M = \exp(1.44 - 0.982 \times \log(352))$$

$$= 0.0133 \qquad \textbf{(A10)}$$

Hoenig (1983) derived Equation **A10** from the regression of 134 stocks among 79 species of fish, molluscs, and cetaceans. Hoenig's regression obtained R^2 = 0.82, but a corresponding coefficient of variation (CV) was not published. An approximate CV of M was estimated by measuring the coordinates off a print of Figure 1 in Hoenig (1983) and repeating the regression. Variability of M was calculated by randomly re-sampling, with replacement, the regression coordinates 10000× and re-computing Equation **A10** for each iteration of the resample. The CV of M from the 10000 random resamples was:

$$CV_M = SD_M / Mean_M$$

$$CV_M = 0.0021 / 0.0134 = 15.46\% \qquad \textbf{(A11)}$$

CV_M over the aggregate number of unassessed days between survey end and commercial season start was then added to the CV of the biomass prior estimate and the CV of variability in vessel catches on start day (Equations **A5-S** and **A5-N**). CV_M was adjusted for the number of unassessed days as:

$$1 - (1 - CV_M)^{\text{no. days}}$$

Total catch by species

Table A1: Total reported catches and discard by taxon during 1st season 2020 C-license fishing, and number of catch reports in which each taxon occurred. Does not include incidental catches of pinnipeds or seabirds.

Species Code	Species / Taxon	Catch Wt. (KG)	Discard Wt. (KG)	N Reports
LOL	*Doryteuthis gahi*	29759086	16614	993
HAK	*Merluccius hubbsi*	255746	8288	765
PAR	*Patagonotothen ramsayi*	145265	145049	926
BAC	*Salilota australis*	92091	1167	207
WHI	*Macruronus magellanicus*	29201	1017	25
CGO	*Cottoperca gobio*	17323	17433	670
RAY	Rajiformes	13823	10133	685
SCA	Scallop	12015	12025	365
GRV	*Macrourus* spp.	5951	2292	125
KIN	*Genypterus blacodes*	4379	595	110
DGH	*Schroederichthys bivius*	3874	4084	457

BLU	*Micromesistius australis*	2340	2282	119
TOO	*Dissostichus eleginoides*	2169	1942	334
GRC	*Macrourus carinatus*	2167	7	7
ING	*Moroteuthis ingens*	1702	1702	242
PTE	*Patagonotothen tessellata*	1410	1410	40
UCH	Sea urchin	1203	1203	91
OCT	*Octopus* spp.	1072	1072	100
SPN	Porifera	188	188	9
MED	Medusae sp.	140	140	11
MAR	*Martialia hyadesi*	135	135	11
MYX	*Myxine* spp.	120	120	22
RED	*Sebastes oculatus*	101	101	16
MUL	*Eleginops maclovinus*	83	83	21
CHE	*Champsocephalus esox*	64	64	21
SAR	*Sprattus fuegensis*	60	60	4
ILL	*Illex argentinus*	55	55	8
EEL	*Iluocoetes fimbriatus*	32	32	16
DGX	Dogfish / Catshark	31	31	2
BUT	*Stromateus brasiliensis*	30	30	6
GRF	*Coelorhynchus fasciatus*	28	28	2
LIT	*Lithodes turkayi*	17	17	2
PAT	*Merluccius australis*	14	14	5
DGS	*Squalus acanthias*	10	10	4
ALF	*Allothunnus fallai*	9	9	1
SEP	*Seriolella porosa*	5	5	3
LIM	*Lithodes murrayi*	4	4	2
MUN	*Munida* spp.	3	3	1
PYM	*Physiculus marginatus*	2	2	1
NEM	*Neophyrnichthys marmoratus*	2	2	1
COP	*Congiopodus peruvianus*	2	2	1
BDU	*Brama dussumieri*	2	2	2
NOW	*Paranotothenia magellanica*	1	1	1
Total		30351955	229453	993